MAXCUTPOOL: DIFFERENTIABLE FEATURE-AWARE MAXCUT FOR POOLING IN GRAPH NEURAL NETWORKS

Anonymous authors
Paper under double-blind review

ABSTRACT

We propose a novel approach to compute the MAXCUT in attributed graphs, *i.e.*, graphs with features associated with nodes and edges. Our approach ~~is robust to the underlying~~ works well on any kind of graph topology and ~~is fully differentiable, making it possible to~~ can find solutions that jointly optimize the MAXCUT along with other objectives. Based on the obtained MAXCUT partition, we implement a hierarchical graph pooling layer for Graph Neural Networks, which is sparse, ~~differentiable~~trainable end-to-end, and particularly suitable for downstream tasks on heterophilic graphs.

1 INTRODUCTION

The MAXCUT is the problem of partitioning the nodes of a graph such that as many edges as possible connect nodes from different sides of the partition. The MAXCUT is orthogonal to the more commonly encountered minCUT, which aims at partitioning the nodes into strongly connected groups. While minCUT is closely related to clustering, MAXCUT relates to the concept of downsampling, *e.g.*, keeping one-every-K, under the assumption that there is a redundancy among the K samples. Like the minCUT, the MAXCUT is a combinatorial optimization problem that, in practice, is approximated by approaches that find suboptimal or unstable solutions for a large class of graphs (Makarychev et al., 2014).

Pooling is ubiquitously used in deep learning for gradually reducing the size of the data while retaining important information. In Convolutional Neural Networks (CNNs), pooling is typically implemented by selecting the maximum within a contiguous patch (*max-pool*) or by computing an average (*avg-pool*). These strategies are naturally related to MAXCUT and minCUT problems, respectively. Similarly to CNNs, Graph Neural Networks (GNNs), which can be seen as a generalization to irregular data, are typically built by alternating Message Passing (MP) and graph pooling layers (Zhou et al., 2020a). A hierarchy of pooling layers gradually extracts global graph properties through the computation of local summaries and is key to building deep GNNs for graph classification (Khasahmadi et al., 2020), node classification (Gao & Ji, 2019; Ma et al., 2020), graph matching (Liu et al., 2021), and spatio-temporal forcasting (Cini et al., 2024; Marisca et al., 2024).

Two important approaches are followed when implementing hierarchical graph pooling. One is to account for the node features with trainable functions that are adapted to a downstream task at hand. The other is to optimize graph theoretical objectives, such as the minCUT or the MAXCUT, to guide the computation of the coarsened graph. Combining the first approach with minCUT objectives is relatively straightforward, as they complement the smoothing effect of MP layers (Hansen & Bianchi, 2023). Conversely, objectives such as MAXCUT that select sparse and uniformly distributed subsamples of nodes have been implemented so far only within non-differentiable frameworks, which account neither for node features nor for task objectives (Luzhnica et al., 2019).

1.1 CONTRIBUTIONS

MAXCUT for attributed graphs. Our first contribution is graph theoretical and consists of a novel GNN-based approach to compute a MAXCUT partition in attributed graphs. Being ~~completely~~ differentiable, our method can be seamlessly integrated into a deep-learning framework where other loss functions can influence the MAXCUT solution. Remarkably, our method is also more robust than traditional approaches in computing the MAXCUT on non-attributed graphs, as it finds a better cut

on most graph topologies. This makes our contribution relevant to *every* application of the MAXCUT problem, such as quantum computing (Zhou et al., 2020b), circuit design (Bashar et al., 2020), statistical physics (Borgs et al., 2012), material science (Liers et al., 2004), computer vision (Abbas & Swoboda, 2022), and quantitative finance (Lee & Constantinides, 2023).

Graph pooling and coarsening. The MAXCUT application we focus on is the problem of learning a coarsened graph within a GNN. In particular, we design a new hierarchical pooling layer that reduces the graph by keeping the nodes from one side of the MAXCUT partition. Our layer is the first to combine a graph theoretical MAXCUT objective with a ~~differentiable and~~ pooling approach that is features-aware ~~approach for pooling~~ and trainable end-to-end. When we include the newly proposed pooling layer in GNNs for graph and node classification, we achieve similar or superior performances compared to state-of-the-art pooling techniques.

Improved scoring-based pooling framework. We propose a simple and efficient scheme to assign node to supernodes when computing the pooled graph. Our scheme can be applied not only to our method but to the whole family of sparse scoring-based graph pooling operators enhancing, in principle, their representational power. Importantly, we bridge the gap between scoring-based and dense pooling methods by using the same operations to compute the features and the topology of the pooled graph.

Heterophilic graph classification dataset. Differently from the existing differentiable pooling operators, the nature of the MAXCUT solution makes our graph pooling operator particularly suitable for heterophilic graphs. While there are benchmark datasets for node classification on heterophilic graphs, there is a lack of such datasets for graph classification. To fill this gap, we introduce a novel synthetic dataset that, to our knowledge, is the first of its kind.

2 Background

2.1 The MAXCUT Problem and the Continuous Relaxations

Let $\mathcal{G} = (\mathcal{V}, \mathcal{E})$ be an undirected graph with non-negative weights on the edges, and let N be the number of nodes in $\mathcal{G}$. A cut in $\mathcal{G}$ is a partition $(\mathcal{S}, \mathcal{V} \setminus \mathcal{S})$ where $\mathcal{S} \subset \mathcal{V}$. The MAXCUT problem consists of finding a cut that maximizes the total volume of edges connecting nodes in $\mathcal{S}$ with those in $\mathcal{V} \setminus \mathcal{S}$. The MAXCUT objective can be expressed as the integer quadratic problem

$$\max_{\boldsymbol{z}} \sum_{i,j \in \mathcal{V}} w_{ij}(1 - z_i z_j) \;\; \text{s.t.} \;\; z_i \in \{-1, 1\}, \tag{1}$$

where $\boldsymbol{z} \in \{-1, 1\}^N$ is an assignment vector indicating to which side of the partition each node is assigned to and w_{ij} is the weight of the edge connecting nodes i and j.

Like other discrete optimization problems of this kind, MAXCUT is NP-hard. The Goeman-Williamson (GW) algorithm (Goemans & Williamson, 1995) provides a semidefinite relaxation of the integer quadratic problem, which makes it tractable:

$$\max_{\boldsymbol{X}} \sum_{i,j \in \mathcal{V}} w_{ij}(1 - \boldsymbol{x}_i \cdot \boldsymbol{x}_j) \;\; \text{s.t.} \;\; \|\boldsymbol{x}_i\| = 1, \tag{2}$$

where $\boldsymbol{X} \in \mathbb{R}^{N \times D}$ is a matrix whose rows are the continuous embeddings of the nodes in $\mathcal{G}$. The vectors $\boldsymbol{X}$ are projected on a random hyperplane to split the nodes and assign them to the two sides of the partition. This algorithm guarantees an expected cut size of .868 of the maximum cut.

Another simple yet effective continuous relaxation is the largest eigenvector vertex selection (LEVS) method (Shuman et al., 2015). Let $\boldsymbol{L}$ be the Laplacian matrix associated to the graph $\mathcal{G}$ and let $\boldsymbol{u}_{\max}$ be the eigenvector of $\boldsymbol{L}$ associated to the largest eigenvalue $\lambda_{\max}$. A cut in $\mathcal{G}$ can be found based on the polarity of the components of $\boldsymbol{u}_{\max}$, for instance by letting $\mathcal{S} = \{i : \boldsymbol{u}_{\max}[i] \geq 0\}$. In the field of graph signal processing, the eigenvectors related to the largest eigenvalues of $\boldsymbol{L}$ are closely related to the operation of high-pass filtering of a graph signal (Tremblay et al., 2018). Specifically, they are used to design graph filters that amplify *high-frequency* components of a signal, *i.e.*, the components that vary the most across adjacent nodes (Shuman et al., 2013).

The MAXCUT problem is closely related to *graph coloring*, which aims at assigning different colors to adjacent nodes. In particular, the 2-color *approximate coloring* (Aspvall & Gilbert, 1984), is the problem of identifying subsets of nodes such that the connections within each subset are minimized. Such coloring is a high-frequency graph signal and induces a partition that is orthogonal with respect to spectral clustering (von Luxburg, 2007).

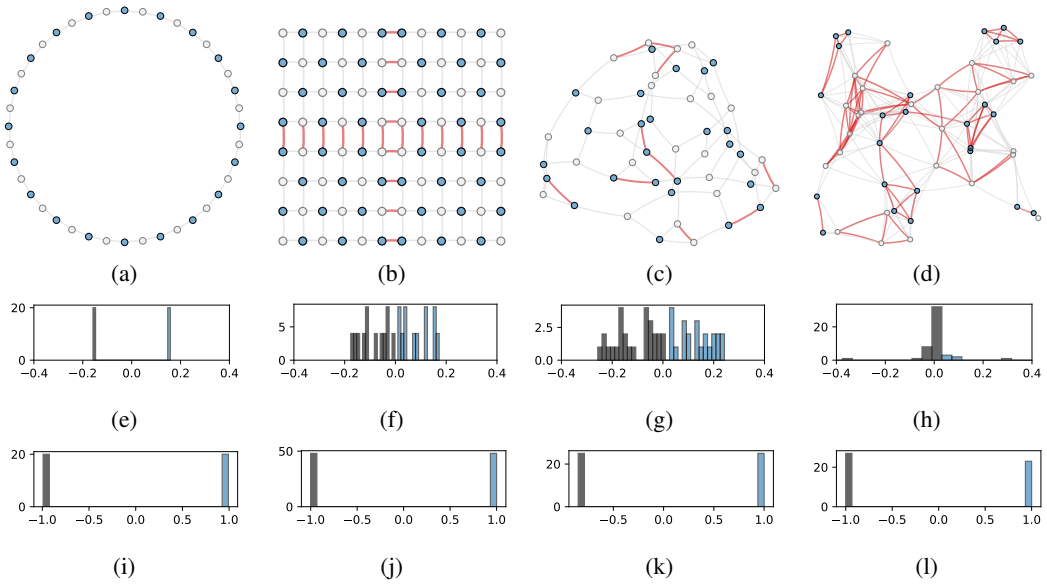

Figure 1: **Top row:** Partitions induced by the sign of the elements in $\boldsymbol{u}_{\max}$. The nodes are colored based on the partition and the red edges are those not cut (the less, the better). **Middle row:** histograms of $\boldsymbol{u}_{\max}$ inducing the partitions above. While in bipartite graphs the separation is sharp, the more a graph is irregular and dense the more the values are clustered around zero, making it difficult to find the optimal MAXCUT. **Bottom row:** histograms of the score vectors generated by our model, which always produce a clear and sharp partition.

A MAXCUT partition that cuts every edge exists only for bipartite graphs. Conversely, in fully connected graphs no more than half of the edges can be cut. Algorithms relying on continuous relaxations to find the MAXCUT partition tend to be unstable and perform poorly, especially as the graph topology departs from the bipartite case (Trevisan, 2009). Fig. 1(a-h) shows the performance of the LEVS method on bipartite and non-bipartite graphs: numerical issues typically occur in more dense and less regular graphs, making it difficult to identify the optimal MAXCUT solution.

2.2 Message passing in GNNs

Let us consider a graph $\mathcal{G} = \left(\boldsymbol{X} \in \mathbb{R}^{N \times F}, \boldsymbol{A} \in \mathbb{R}^{N \times N}\right)$. A basic MP operator can be described as

$$\boldsymbol{X}' = \sigma\left(\boldsymbol{P}\boldsymbol{X}\boldsymbol{\Theta}\right) \tag{3}$$

where σ is a non linear activation function, $\boldsymbol{\Theta}$ are trainable parameters, and $\boldsymbol{P}$ is a propagation operator matching the sparsity pattern of $\boldsymbol{A}$. Each MP layer relies on a specific propagation operator. For instance, in Graph Convolutional Networks (GCNs) (Kipf & Welling, 2017), the propagation operator is defined as $\boldsymbol{P} = \hat{\boldsymbol{D}}^{-\frac{1}{2}}\hat{\boldsymbol{A}}\hat{\boldsymbol{D}}^{-\frac{1}{2}}$, where $\hat{\boldsymbol{A}} = \boldsymbol{A} + \boldsymbol{I}$ and $\hat{D}_{ii} = \sum_{j=0} \hat{\boldsymbol{A}}_{ij}$.

Due to the fixed, non-negative smoothing nature of most propagation operators, the repeated application of $\boldsymbol{P}$ can lead to over-smoothing. If that happens, the feature representations of nodes become increasingly similar, hindering the function approximation capabilities of a GNN, which can only learn smooth graph signals (Wu et al., 2019; Wang et al., 2019). In contrast, by ~~using a *sharpening* propagation operator~~combining smoothing propagation operators with *sharpening* ones, any kind of gradients can be learned (Eliasof et al., 2023). Since there is no universal definition for such an operator, we rely on the formulation introduced by Bianchi (2022):

$$\boldsymbol{P} = \boldsymbol{I} - \delta\left(\boldsymbol{I} - \boldsymbol{D}^{\frac{1}{2}}\boldsymbol{A}\boldsymbol{D}^{\frac{1}{2}}\right) = \boldsymbol{I} - \delta\boldsymbol{L}^{\text{sym}} \tag{4}$$

where δ is a smoothness hyperparameter and $\boldsymbol{L}^{\text{sym}}$ is the symmetrically normalized Laplacian of $\mathcal{G}$. As observed by Bianchi (2022), when $\delta = 0$ the MP behaves like a simple Multilayer Perceptron (MLP). Instead, when $\delta = 1$ the behavior is close to that of a GCN. Finally, as noted by Eliasof et al. (2023), when $\delta > 1$ the propagation operator favors the realization of non-smooth signals on the graph and we refer to this variant as a Heterophilic Message Passing (HetMP) operator. We note that this can be seen as ~~a graph-equivalent~~ the graph counterpart of the Laplacian sharpening kernels for images, mapping connected nodes to different values (Mather & Koch, 2022).

2.3 Graph pooling

While there are profound differences between existing graph pooling approaches, most of them can be expressed through the Select-Reduce-Connect (SRC) framework (Grattarola et al., 2022). Specifically, a pooling operator $\texttt{POOL} : (\boldsymbol{A}, \boldsymbol{X}) \mapsto (\boldsymbol{A}', \boldsymbol{X}')$ can be expressed as the combination of three sub-operators:

- $\texttt{SEL} : (\boldsymbol{A}, \boldsymbol{X}) \mapsto \boldsymbol{S} \in \mathbb{R}^{N \times K}$, is a selection operator that defines how the N original nodes are mapped to the K pooled nodes, called *supernodes*, being $\boldsymbol{S}$ the *selection matrix*.
- $\texttt{RED} : (\boldsymbol{X}, \boldsymbol{S}) \mapsto \boldsymbol{X}' \in \mathbb{R}^{K \times F}$, is a reduction operator that yields the features of the supernodes. A common way to implement $\texttt{RED}$ is $\boldsymbol{X}' = \boldsymbol{S}^\top \boldsymbol{X}$.
- $\texttt{CON} : (\boldsymbol{A}, \boldsymbol{S}) \mapsto \boldsymbol{A}' \in \mathbb{R}_{\geq 0}^{K \times K}$, is a connection operator that generates the new adjacency matrix and, potentially, edge features. Typically, $\texttt{CON}$ is implemented as $\boldsymbol{A}' = \boldsymbol{S}^\top \boldsymbol{A} \boldsymbol{S}$ or $\boldsymbol{A}' = \boldsymbol{S}^+ \boldsymbol{A} \boldsymbol{S}$.

Different design choices for $\texttt{SEL}$, $\texttt{RED}$, and $\texttt{CON}$ induce a taxonomy of the operators. For example, if $\texttt{SEL}$, $\texttt{RED}$, and $\texttt{CON}$ are learned end-to-end the pooling operators are called *trainable*, *non-trainable* otherwise. Relevant to this work, are the families of pooling methods described in the following.

Soft-clustering methods, sometimes referred to as *dense* (Grattarola et al., 2022), assign each node to more than one supernode through a soft membership. Representatives methods such as DiffPool (Ying et al., 2018), MinCutPool (Bianchi et al., 2020a), StructPool (Yuan & Ji, 2020), HoscPool (Duval & Malliaros, 2022), and Deep Modularity Networks (DMoN) (Tsitsulin et al., 2023), compute a soft cluster assignment matrix $\boldsymbol{S} \in \mathbb{R}^{N \times K}$ either with an MLP or an MP-layer operating on node the features and followed by a $\texttt{softmax}$. Each method leverages different unsupervised auxiliary loss functions to guide the formation of the clusters. Trainable soft-clustering methods usually perform well on downstream tasks due to their flexibility and *expressive power*, which is the capability of retaining all the information from the original graph (Bianchi & Lachi, 2023). However, storing the soft assignments $\boldsymbol{S}$ is a memory bottleneck for large graphs (see, *e.g.*, the analysis of memory usage in Appendix F.3) and soft memberships cause pooled graphs to be very dense and not interpretable. Additionally, each graph is mapped to the same fixed number of supernodes K, which can hinder the generalization capabilities in datasets where the size of each graph varies significantly.

Scoring-based methods select supernodes from the original nodes based on a node scoring vector $\boldsymbol{s}$. The chosen nodes correspond to the top K elements of $\boldsymbol{s}$, where K can be a ratio of the nodes in each graph, making these methods adaptive to graph size. Representatives such as Top-k Pooling (Top-k) (Gao & Ji, 2019; Knyazev et al., 2019), ASAPool (Ranjan et al., 2020), SAGPool (Lee et al., 2019), PanPool (Ma et al., 2020), TAPool (Gao et al., 2021), CGIPool (Pang et al., 2021), and IPool (Gao et al., 2022) primarily differ in how they compute the scores or in the auxiliary tasks they optimize to improve the quality of the pooled graph. Despite a few attempts to encourage diversity among the selected nodes (Zhang et al., 2019; Noutahi et al., 2019), scoring-based methods derive the scores from node features that tend to be locally similar, especially after being transformed by MP operations. As such, the pooled graph often consists of a chunk of strongly connected nodes that possess similar characteristics. Consequently, entire sections of the graph are usually not represented, leading to reduced expressiveness and lower performance in downstream tasks (Wang et al., 2024).

One-every-$\boldsymbol{K}$ methods leverage graph-theoretical properties to select supernodes by subsampling the graph uniformly. For instance, k Maximal Independent Sets Pooling (k-MIS) (Bacciu et al., 2023) identifies as supernodes the members of a maximal K-independent set, *i.e.*, nodes separated by at least K-hops on the graph. Graclus (Dhillon et al., 2007; Defferrard et al., 2016) creates supernodes by merging the pairs of most connected nodes in the graph. SEP (Wu et al., 2022) partitions the node hierarchically according to a precomputed tree that minimizes the structural entropy of the graph.

Node Decimation Pooling (NDP) (Bianchi et al., 2020b) divides the graph into two sets, $\mathcal{V}_+$ and $\mathcal{V}_-$, according to the partition induced by the components of $\boldsymbol{u}_{\max}$ (see Section 2.1). One of the two sides of the partition is dropped ($\mathcal{V}_-$), while the other ($\mathcal{V}_+$) becomes the set of supernodes. While both Graclus and NDP can only reduce the number of nodes by approximately half, higher pooling ratios (one-every-2^K) are achieved by applying them recursively K times. Nevertheless, they lack the same control of soft-clustering and scoring-based methods in fixing the size of the pooled graphs. Like the scoring-based methods, one-every-K methods are adaptive and produce crisp cluster assignments. However, they are not trainable and precompute the pooled graph based on the topology without accounting for the node features or the downstream task. Tab. 1 summarizes the drawbacks of the existing families of pooling methods.

Table 1: Drawbacks of different types of pooling operators.

Soft-clustering	**Score-based**	**One-every-K**
✗ Not adaptive to graph size	✗ Pooling not uniform	✗ Limited flexibility
✗ Dense and not interpretable pooled graphs	✗ Not expressive	✗ Features agnostic
✗ High memory cost	✗ Worse performance	✗ Task agnostic

3 METHOD

We leverage a GNN to generate a MAXCUT partition while accounting for node features and additional objectives from a downstream task. In particular, we let node features and task-specific losses influence the selection of the MAXCUT solution, creating partitions that not only maximize the number of cut edges but also prioritize nodes that are optimal for the downstream task. To reach this goal, it is necessary to overcome a tension between the effect of a standard MP layer and the MAXCUT: the first applies a smoothing operation that makes adjacent nodes as similar as possible, which is orthogonal to the objective of the latter. Therefore, to implement MAXCUT with a GNN we rely on HetMP, implemented by setting $\delta > 1$ in the MP operation in Eq. 4. As discussed in Sec. 2.1, solving the MAXCUT problem is equivalent to coloring adjacent nodes differently. Notably, this is an intrinsic effect of HetMP that makes features of adjacent nodes as different as possible, effectively acting as a high-pass filter. Therefore, optimizing a MAXCUT loss on features generated by HetMP layers addresses the limitation of traditional scoring-based methods that compute the scores from features produced by homogeneous MP operations.

The layer we propose is called MaxCutPool and we present it through the SRC framework. The SEL operation in MaxCutPool identifies as supernodes a subset $\mathcal{S}$ of the nodes in the original graph. An auxiliary GNN, called *ScoreNet*, consists of a stack of HetMP layers that map the node features into a vector $\boldsymbol{s} = \text{ScoreNet}(\boldsymbol{X}, \boldsymbol{A}) \in [-1, 1]^N$ that assigns a score to each node. The indices $\boldsymbol{i} = \text{top}_K(\boldsymbol{s})$ associated with the highest scores identify the K supernodes. Additional details about the ScoreNet are in Appendix C.1. Fig. 1(i-l) shows the histograms of the score vectors $\boldsymbol{s}$ generated by the ScoreNet for the 4 example graphs. Compared to the histograms of $\boldsymbol{u}_{\max}$ in Fig. 1(e-h), the values in $\boldsymbol{s}$ always follow a distribution with two sharp and well-separated modes, yielding a clear node partition.

After the K supernodes are selected, the remaining $N-K$ nodes are assigned to one of the supernodes via the nearest neighbor aggregation. An assignment matrix $\boldsymbol{S}$ is built by performing a ~~breadth first~~ breadth-first visit of the graph where, starting from the supernodes, all the remaining nodes are assigned to their nearest supernode (see Figure 2). More formally, the assignment matrix $\boldsymbol{S}$ is defined as

$$\texttt{SEL} : [\boldsymbol{S}]_{ij} = 1 \iff j = \phi(\mathcal{S}, \boldsymbol{A}, i),$$

where $\phi(\mathcal{S}, \boldsymbol{A}, i)$ returns the nearest supernode of node i. The visit of the graph is iterated until all nodes are assigned to a supernode or until a maximum number of iterations is reached. In the latter case, nodes that are still unassigned are assigned at random, which ensures that the pooled graph is always connected. Keeping the maximum number of iterations small (*e.g.*, 2 or 3) prevents pointless attempts to reach a supernode, *e.g.*, when there are no supernodes within a disconnected graph component, and also injects randomness acting as a regularizer that helps to move away from suboptimal configurations often encountered at the beginning of the training stage. The pseudo-code for a GPU parallel implementation of the proposed assignment scheme is in Appendix A.

The RED operation for computing the features of the supernodes can be implemented in two ways:

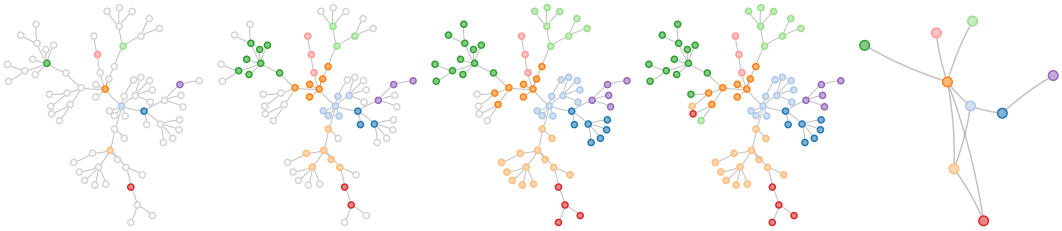

(a) (b) (c) (d) (e)

Figure 2: **(a)** The nodes with the $K = 9$ highest scores are selected. **(b-c)** Their ID is propagated to the unselected nodes until all are covered or until a maximum number of iterations (2 here) is reached. **(d)** The 4 remaining nodes are assigned randomly. **(e)** The pooled graph is obtained by aggregating the nodes with the same ID and coalescing the edges connecting nodes from different groups.

$$\texttt{RED}: \cancel{[\boldsymbol{X}']_{i:} = s_i \odot [\boldsymbol{X}]_{i:}}\ \boldsymbol{X}' = s_i \odot [\boldsymbol{X}]_i \quad \text{or} \quad \texttt{RED}: \cancel{\boldsymbol{X}' = \boldsymbol{s} \odot \boldsymbol{S}^\top \boldsymbol{X}}\ \boldsymbol{X}' = \boldsymbol{s}_i \odot \boldsymbol{S}^\top \boldsymbol{X}.$$

The Hadamard product $\odot$ enables gradients flowing through the ScoreNet during back-propagation, making it possible for the gradients of the task loss to reach every component of our model, despite the non-differentiable top$_K$ operation. When the first and second options are used to implement RED, we refer to the pooling operator as MaxCutPool and MaxCutPool-E, respectively. The suffix "-E" indicates the pooling operator satisfies the sufficient conditions for expressiveness defined by Bianchi & Lachi (2023).

Finally, having defined a cluster assignment matrix $\boldsymbol{S}$, the CON operation can be implemented as

$$\texttt{CON}: \boldsymbol{A}' = \boldsymbol{S}^\top \boldsymbol{A} \boldsymbol{S}.$$

3.1 Auxiliary Loss

Each MaxCutPool layer is associated with an auxiliary loss that encourages the top-K selected nodes to belong to the same side of the MAXCUT partition. The loss is defined as:

$$\mathcal{L}_{\text{cut}} = \frac{\boldsymbol{s}^\top A \boldsymbol{s}}{|E|} \tag{5}$$

where $|E| = \sum_{ij} w_{ij}$ is the total edge weight of the graph. Since $-1 \leq s_i \leq 1$, we have $-|E| \leq \boldsymbol{s}^\top A \boldsymbol{s} \leq |E|$, hence $-1 \leq \mathcal{L}_{\text{cut}} \leq 1$. This loss evaluates the ratio between the volume of the cut and the total volume of the edges. Minimizing $\mathcal{L}_{\text{cut}}$ encourages the nodes to be assigned to different partitions if and only if they are connected. The loss reaches its minimum -1 when all connected nodes are assigned to opposite sides of the partition, *i.e.*, when all the edges are cut. Clearly, this can happen only in bipartite graphs. The details about the derivation of the loss are in Appendix B.

A GNN model consisting of MP layers interleaved with MaxCutPool layers can be trained end-to-end to jointly minimize a task loss $\mathcal{L}_{\text{task}}$ and the auxiliary loss $\mathcal{L}_{\text{cut}}$. The total loss is then defined as

$$\mathcal{L} = \mathcal{L}_{\text{task}} + \sum_l \beta \mathcal{L}_{\text{cut}}^{(l)} \tag{6}$$

where β is a scalar weighting each auxiliary loss $\mathcal{L}_{\text{cut}}^{(l)}$ associated with the l-th MaxCutPool layer.

3.2 Homophilic and Heterophilic Operations

Despite the presence of HetMP layers and the heterophilic loss, MaxCutPool can be inserted into GNNs equipped with traditional MP layers. In fact, the homophilic nature of the latter is leveraged by our method. After a standard homophilic MP, the stronger the association between a pair of nodes, the more similar their features will be. Keeping them both will, thus, be redundant, and one of them can be dropped. This is precisely what is done by SEL that, thanks to its heterophilic design, samples nodes with few direct links that are uniformly distributed over the graph.

MaxCutPool contains an additional homophilic operation: computing the assignments $\boldsymbol{S}$ through the nearest-neighbor aggregation, which synergizes with the uniform sampling of the supernodes. The assignments are used by CON to produce a connectivity matrix that is connected yet sparse and they can also be leveraged by RED to ensure the expressiveness of the pooling layer. However, for heterophilic datasets, where such a homophilic assignment might not be appropriate, the non-expressive variant of our method offers a more suitable alternative.

In general, rather than creating tension, combining homophilic and heterophilic components provides a GNN with MaxCutPool the flexibility for handling different scenarios. As we show in the experimental evaluation, our model can even switch to a completely homophilic setting by adjusting the values of δ and β, or by ignoring the auxiliary loss.

3.3 Relation with other pooling methods

MaxCutPool belongs to the scoring-based pooling family from which inherits the possibility of specifying any desired pooling ratio adaptable to the size N_i of the i-th graph, *i.e.*, ~~$K^{(i)} = \lfloor N^{(i)} * 0.5 \rfloor$. Differently from the other scoring-based methods and thanks to the HetMP layers, MaxCutPool selects supernodes that are not concentrated in the same section of the graph but are, instead, distributed more uniformly over the whole graph, which is similar to the~~ $K_i = \lfloor N_i * 0.5 \rfloor$, while achieving node selection patterns similar to one-over-K methods. In methods like k-MIS the flexibility provided by trainable functions is only used to choose between a small set of maximal solutions that do not break the hard constraint of the supernodes to be K-independent. On the other hand, in MaxCutPool any set of supernodes can, in principle, be chosen making MaxCutPool more flexible and able to better adapt to the requirements of the downstream task. Finally, MaxCutPool is the only scoring-based pooler with a graph-theoretical auxiliary regularization loss.

The proposed method for constructing the cluster assignment matrix $\boldsymbol{S}$ from the selected supernodes can be applied to other scoring-based pooling methods. This naturally enhances their expressiveness by enabling the use of the same CON and RED operations adopted by soft-clustering approaches, which retains all the information from the original graph. By addressing the key limitation in the expressiveness of scoring-based pooling methods, our approach retains the benefits of sparsity and interpretability of scoring-based poolers while narrowing the gap with soft-clustering methods.

4 Experimental evaluation

We consider three different tasks to demonstrate the effectiveness of MaxCutPool. The code to reproduce the reported results in publicly available[1]. The details about the architectures used in each experiment and the hyperparameters selection procedure are described in Appendix C.

4.1 Computation of the MAXCUT partition

~~This experiment focuses on computing~~ The main focus of this experiment is to evaluate the capability of the proposed loss $\mathcal{L}_{\text{cut}}$ to optimize the MAXCUTobjective, despite the potential risks of getting stuck in local minima due to its gradient-based nature. We compute a MAXCUT partition by training a simple GNN consisting of a MP layer followed by MaxCutPool and trained by minimizing only the loss in Eq. 5 (details in Appendix C.2). We use a Graph Isomorphism Network (GIN) layer (Xu et al., 2019) as the MP layer. We compare our model against the LEVS approach based on $\boldsymbol{u}_{\max}$, the GW algorithm, and a GNN with GCN layers that minimize a MAXCUT loss, as proposed by Schuetz et al. (2022). For a fair comparison, ours and this GNN architecture have a comparable number of learnable parameters.

We considered 9 graphs generated via the PyGSP library (Defferrard et al., 2017), including bipartite graphs such as the Grid2D and Ring, and 7 graphs from the GSet dataset (Ye, 2003), including random, planar, and toroidal graphs, typically used as benchmark for evaluating MAXCUT algorithms (details in App. D.1). Results are shown in Tab. 2. Performance is computed in terms of the percentage of cut edges: the higher, the better. With one exception, MaxCutPool always finds the best cut.

[1] https://anonymous.4open.science/r/MaxCutPool

Table 2: Size of the graph cuts obtained with MaxCutPool, a GNN with GCN layers, and two common algorithms to compute the MAXCUT. GW results are absent for some entries of the PyGSP datasets and for GSet because the solver failed to converge.

(a) PyGSP datasets

Dataset	GW	NDP	GCN	MaxCutPool
BarabasiAlbert	0.6875	0.6589	0.7240	**0.7292**
Community	0.6767	0.6429	0.6805	**0.6814**
ErdősRenyi	0.6920	0.6858	0.6797	**0.7105**
Grid (10×10)	**1.0000**	**1.0000**	0.9222	**1.0000**
Grid (60×40)	-	0.9787	0.1862	**0.9815**
Minnesota	-	0.9104	0.8904	**0.9130**
RandRegular	0.4827	0.8760	0.8733	**0.9040**
Ring	**1.0000**	**1.0000**	0.4200	**1.0000**
Sensor	0.6000	0.5719	0.6281	**0.6406**

(b) GSet datasets

Dataset	NDP	GCN	MaxCutPool
G14	0.6155	0.6323	**0.6412**
G15	0.5945	0.6288	**0.6424**
G22	0.6441	0.6409	**0.6577**
G49	**1.0000**	0.9683	**1.0000**
G50	**0.9800**	0.9610	0.9750
G55	0.7568	0.7865	**0.8068**
G70	0.8803	0.8945	**0.9086**

4.2 GRAPH CLASSIFICATION

For this task, we evaluate the classification accuracy of a GNN classifier with the following structure: MP(32)-Pool-MP(32)-Readout, using GIN as the MP layer. The Pool operation is implemented either by MaxCutPool or by the following competing methods: Diffpool (Ying et al., 2018), DMoN (Tsitsulin et al., 2023), MinCutPool (Bianchi et al., 2020a), Top-k (Gao & Ji, 2019), Graclus (Dhillon et al., 2007), k-MIS (Bacciu et al., 2023). We also consider Edge-Contraction Pooling (ECPool) (Diehl, 2019) that pools the graph by contracting the edge connecting similar nodes. For MaxCutPool, we evaluate three variants: (i) MaxCutPool, the standard version; (ii) MaxCutPool-E, the variant with expressive CON; (iii) MaxCutPool-NL, where "NL" stands for "no loss", meaning we do not optimize the auxiliary loss in the GNN. This serves as an ablation study to assess the importance of the auxiliary loss. Whenever edge attributes are available, the first GIN layer is replaced by a GINE layer (Hu et al., 2020), which takes into account edge attributes. Further implementation details are in Appendix C.3.

As graph classification datasets we consider 8 TUD datasets (COLLAB, DD, NCI1, ENZYMES, MUTAG, Mutagenicity, PROTEINS, and REDDIT-BINARY) (Morris et al., 2020), the Graph Classification Benchmark Hard (GCB-H) (Bianchi et al., 2022), and EXPWL1 (Bianchi & Lachi, 2023), which is a recent dataset for testing the expressive power of GNNs. In addition, we introduce a novel dataset consisting of $5,000$ multipartite graphs: each graph is complete 10-partite, meaning that the nodes can be partitioned into 10 groups so that the nodes in each group are disconnected, but are connected to all the nodes of the other groups. To the best of our knowledge, this is the first benchmark dataset for graph classification with heterophilic graphs. While the Multipartite dataset consists of complex graph structures, the classification label is determined solely by the node features, allowing us to assess whether the GNN can effectively isolate relevant information despite the presence of misleading topological information. The construction of the Multipartite dataset and a further discussion about its properties are reported in Appendix D.2.

Whenever the node features were not available, we used node labels. If node labels were also unavailable, we used a constant as a surrogate node feature. Further details about the remaining datasets can be found in Appendix D.3. The datasets were split via a 10-fold cross-validation procedure. The training dataset was further partitioned into a 90-10% train-validation random split. This approach is similar to the procedure described by Errica et al. (2020). Each model was trained for $1,000$ epochs with early stopping, keeping the checkpoint with the best validation accuracy.

The results are reported in Tab. 3. For completeness, we also reported the performance of the same GNN model without pooling layers ("No pool"). We conducted a preliminary ANOVA test (p-value 0.05) for each dataset followed by a pairwise Tukey-HSD test (p-value 0.05) to group models whose performance is not significantly different. Those belonging to the top-performing group are colored in green. The ANOVA test failed on ENZYMES, PROTEINS, MUTAG, and DD, meaning that the

Table 3: Mean and standard deviations of the graph classification accuracy. For each dataset the best performing method and those that are not significantly different from it are colored in green. If a method is in the top-performing group is assigned with a score of 1, 0 otherwise.

Pooler	GCB-H	COLLAB	EXPWL1	Mult.	Mutag.	NCI1	REDDIT-B	Score
No pool	$74_{\pm 4}$	$74_{\pm 2}$	$87_{\pm 2}$	$14_{\pm 12}$	$79_{\pm 2}$	$78_{\pm 3}$	$90_{\pm 2}$	-
DiffPool	$51_{\pm 8}$	$70_{\pm 2}$	$69_{\pm 3}$	$9_{\pm 1}$	$78_{\pm 2}$	$75_{\pm 2}$	$90_{\pm 2}$	1
DMoN	$74_{\pm 3}$	$68_{\pm 2}$	$73_{\pm 3}$	$52_{\pm 2}$	$80_{\pm 2}$	$77_{\pm 2}$	$88_{\pm 2}$	3
EdgePool	$75_{\pm 4}$	$72_{\pm 3}$	$90_{\pm 2}$	$55_{\pm 3}$	$80_{\pm 2}$	$77_{\pm 3}$	$91_{\pm 2}$	4
Graclus	$75_{\pm 3}$	$72_{\pm 3}$	$90_{\pm 2}$	$25_{\pm 18}$	$80_{\pm 2}$	$77_{\pm 2}$	$90_{\pm 3}$	4
k-MIS	$75_{\pm 4}$	$71_{\pm 2}$	$99_{\pm 1}$	$58_{\pm 2}$	$79_{\pm 2}$	$75_{\pm 3}$	$90_{\pm 2}$	4
MinCutPool	$75_{\pm 5}$	$70_{\pm 2}$	$71_{\pm 3}$	$56_{\pm 3}$	$78_{\pm 3}$	$73_{\pm 3}$	$87_{\pm 2}$	1
Top-k	$56_{\pm 5}$	$72_{\pm 2}$	$73_{\pm 2}$	$43_{\pm 3}$	$75_{\pm 3}$	$73_{\pm 2}$	$77_{\pm 2}$	0
MaxCutPool	$73_{\pm 3}$	$77_{\pm 2}$	$100_{\pm 0}$	$90_{\pm 2}$	$77_{\pm 2}$	$75_{\pm 2}$	$89_{\pm 3}$	5
MaxCutPool-E	$74_{\pm 3}$	$77_{\pm 2}$	$100_{\pm 0}$	$87_{\pm 5}$	$79_{\pm 1}$	$76_{\pm 2}$	$89_{\pm 2}$	7
MaxCutPool-NL	$61_{\pm 6}$	$77_{\pm 3}$	$100_{\pm 0}$	$91_{\pm 1}$	$76_{\pm 3}$	$74_{\pm 2}$	$86_{\pm 3}$	3

difference in the performance of the GNNs equipped with different poolers is not significant. For this reason, the results on these datasets are omitted from Tab. 3 and reported in Appendix E.1.

MaxCutPool consistently ranks among the top-performing methods across all evaluated datasets. Notably, on the EXPWL1 even the non-expressive variant of MaxCutPool achieves a perfect accuracy (100%), outperforming the competitors. This is the first known ~~instance~~ example of a non-expressive pooler passing the expressiveness test provided by this dataset~~, serving as a counterexample to Theorem 1 in Bianchi & Lachi (2023).~~ On the Multipartite dataset, MaxCutPool performs significantly better than every pooling method. When compared to the "No pool" baseline, on most datasets MaxCutPool improves the classification performance by increasing the receptive field of the MP layers while retaining only the necessary information and enhancing the overall expressive power of the GNN model. It is worth noting that the EXPWL1 and Multipartite are the least homophilic datasets (see Appendix D.3), indicating that MaxCutPool is particularly effective for heterophilic graphs. On the COLLAB dataset, all MaxCutPool variants achieve the top accuracy of 77%, showing a statistically significant improvement over other methods. Notably, in the MaxCutPool and MaxCutPool-E variants the auxiliary loss term plateaued around 0, making them equivalent to the MaxCutPool-NL variant that, in this case, achieves the same performance. This indicates that our method remains robust even when the auxiliary loss is not needed for the downstream task. Overall, the MaxCutPool-E variant, which satisfies expressiveness conditions, exhibits similar or better performance compared to MaxCutPool across most datasets. In contrast, the performance decline observed in the MaxCutPool-NL variant demonstrates the importance of the auxiliary loss.

4.3 Node classification

For this task, we adopted a simple auto-encoder architecture for node classification: MP(32)-Pool-MP(32)-Unpool-MP(32)-Readout, with GIN as MP. The Unpool operation (also referred to as *lifting* (Jin et al., 2020)) is implemented by copying in each node i the value of the supernode j to which the i was assigned by the `SEL` operation in the pooling phase. Zero-padding is used when lifting nodes not assigned to any supernode, like in the case of Top-k. Further details about the architecture for node classification and the unpooling procedure are deferred to Appendix C.4.

For this experiment, we considered the 5 heterophilic datasets presented in Platonov et al. (2023) (details in Appendix D.4). As pooling methods we considered Top-k (Gao & Ji, 2019), k-MIS (Bacciu et al., 2023), NDP (Bianchi et al., 2020b), and MaxCutPool. We did not consider Graclus or any soft-clustering poolers, as they were exhausting the RAM and GPU VRAM, respectively, given the large size of the graphs. On the other hand, MaxCutPool is very parsimonious in terms of computational resources and scales very well with the graph size. To systematically estimate the space complexity of the different pooling methods we performed an experimental evaluation of the GPU VRAM usage, which can be found in Appendix F.3.

Following Platonov et al. (2023), in Tab. 4 we report the means and standard deviations of the accuracy for Roman-empire and Amazon-ratings, and of the ROC AUC for Tolokers, Minesweeper, and Questions. The results are computed on the 10 public folds of these datasets. When configured

Table 4: Node classification accuracy (Roman-empire, Amazon-ratings) and AUROC (Minesweeper, Tolokers, Questions). The best performing models in each dataset are in green and get 1 score point, 0 otherwise.

Pooler	**Roman-e.**	**Amazon-r.**	**Minesw.**	**Tolokers**	**Questions**	**Score**
No pool	*$59_{\pm 0}$*	*$46_{\pm 1}$*	*$86_{\pm 2}$*	*$86_{\pm 4}$*	*$71_{\pm 2}$*	-
Top-k	$26_{\pm 7}$	$46_{\pm 4}$	$94_{\pm 1}$	$89_{\pm 5}$	$64_{\pm 3}$	1
k-MIS	$23_{\pm 3}$	$48_{\pm 2}$	$75_{\pm 2}$	$84_{\pm 2}$	$83_{\pm 1}$	1
NDP	$22_{\pm 5}$	$53_{\pm 2}$	$98_{\pm 0}$	$88_{\pm 6}$	$68_{\pm 4}$	3
MaxCutPool	$56_{\pm 3}$	$53_{\pm 1}$	$96_{\pm 1}$	$87_{\pm 3}$	$82_{\pm 4}$	4
MaxCutPool-E	$60_{\pm 4}$	$53_{\pm 2}$	$97_{\pm 1}$	$91_{\pm 2}$	$85_{\pm 5}$	**5**

with MaxCutPool and MaxCutPool-E, the node classification architecture achieves significantly superior performance on the Roman-Empire dataset, which is notably the most heterophilic among all the datasets (see Tab. 11). On the remaining datasets, our method performs well overall. Unlike the other pooling methods that achieve top performance only on a subset of the datasets, MaxCutPool-E is consistently in the top tier.

5 Conclusion

This work contributes significantly to both the `MAXCUT` optimization and the development of specialized GNN architectures to solve combinatorial optimization problems. Our proposed GNN-based `MAXCUT` algorithm not only extends the `MAXCUT` optimization to attributed graphs and combines it with task-specific losses but also surpasses the performances of traditional methods on non-attributed graphs. While a conventional GNN with a huge capacity manages to optimize a `MAXCUT` loss (Schuetz et al., 2022), our model is much more efficient thanks to the Heterophilic Message Passing layers. This results highlight the importance of aligning the GNN architecture with the problem's inherent structure: in this case, leveraging heterophilic propagation to solve problems that seek dissimilarity between neighboring nodes.

Our second contribution is to utilize the proposed `MAXCUT` optimizer to implement a graph pooling method that combines the flexibility of soft-clustering approaches with the efficiency of scoring-based methods and with the theoretically-inspired design of one-every-K strategies. GNNs for graph and node classification equipped with our proposed pooling layer consistently achieves superior performance across diverse downstream tasks. Differently from existing graph pooling and graph coarsening approaches that aim at preserving low-frequencies on the graph (Loukas, 2019), our method performs exceptionally well also on heterophilic datasets. While our pooling layer can implement any pooling ratio, the auxiliary loss is optimized for the node partition induced by the `MAXCUT`, whose size might not be aligned with the specified pooling ratio. When the distribution of the nodes' degree is approximately uniform, the `MAXCUT` induces an approximately balanced partition corresponding to a pooling ratio of ≈ 0.5, which is, thus, generally a good choice.

Looking forward, we see great potential in pretraining GNNs with auxiliary losses. This aligns with the principles of foundational models (Bommasani et al., 2021) and could facilitate the development of more effective and general-purpose graph pooling techniques.

References

Ahmed Abbas and Paul Swoboda. Rama: A rapid multicut algorithm on gpu. In *Proceedings of the IEEE/CVF Conference on Computer Vision and Pattern Recognition*, pp. 8193–8202, 2022.

Bengt Aspvall and John R. Gilbert. Graph coloring using eigenvalue decomposition. *SIAM Journal on Algebraic Discrete Methods*, 5(4):526–538, 1984.

Davide Bacciu, Alessio Conte, and Francesco Landolfi. Graph pooling with maximum-weight k-independent sets. In *Thirty-Seventh AAAI Conference on Artificial Intelligence*, 2023.

Mohammad Khairul Bashar, Antik Mallick, Daniel S. Truesdell, Benton H. Calhoun, Siddharth Joshi, and Nikhil Shukla. Experimental demonstration of a reconfigurable coupled oscillator platform to solve the max-cut problem. *IEEE Journal on Exploratory Solid-State Computational Devices and Circuits*, 6(2):116–121, 2020. doi: 10.1109/JXCDC.2020.3025994.

Filippo Maria Bianchi. Simplifying clustering with graph neural networks. *arXiv preprint arXiv:2207.08779*, 2022.

Filippo Maria Bianchi and Veronica Lachi. The expressive power of pooling in graph neural networks. In *Advances in Neural Information Processing Systems*, volume 36, pp. 71603–71618, 2023.

Filippo Maria Bianchi, Daniele Grattarola, and Cesare Alippi. Spectral clustering with graph neural networks for graph pooling. In *International conference on machine learning*, pp. 874–883. PMLR, 2020a.

Filippo Maria Bianchi, Daniele Grattarola, Lorenzo Livi, and Cesare Alippi. Hierarchical representation learning in graph neural networks with node decimation pooling. *IEEE Transactions on Neural Networks and Learning Systems*, 33(5):2195–2207, 2020b.

Filippo Maria Bianchi, Claudio Gallicchio, and Alessio Micheli. Pyramidal reservoir graph neural network. *Neurocomputing*, 470:389–404, 2022. ISSN 0925-2312. doi: https://doi.org/10.1016/j.neucom.2021.04.131.

Derrick Blakely, Jack Lanchantin, and Yanjun Qi. Time and space complexity of graph convolutional networks. *Accessed on: Dec*, 31:2021, 2021.

Rishi Bommasani, Drew A Hudson, Ehsan Adeli, Russ Altman, Simran Arora, Sydney von Arx, Michael S Bernstein, Jeannette Bohg, Antoine Bosselut, Emma Brunskill, et al. On the opportunities and risks of foundation models. *arXiv preprint arXiv:2108.07258*, 2021.

Christian Borgs, Jennifer T Chayes, László Lovász, Vera T Sós, and Katalin Vesztergombi. Convergent sequences of dense graphs ii. multiway cuts and statistical physics. *Annals of Mathematics*, pp. 151–219, 2012.

Eli Chien, Jianhao Peng, Pan Li, and Olgica Milenkovic. Adaptive universal generalized pagerank graph neural network. In *International Conference on Learning Representations*, 2021.

Andrea Cini, Danilo Mandic, and Cesare Alippi. Graph-based Time Series Clustering for End-to-End Hierarchical Forecasting. *International Conference on Machine Learning*, 2024.

Michaël Defferrard, Xavier Bresson, and Pierre Vandergheynst. Convolutional neural networks on graphs with fast localized spectral filtering. *Advances in neural information processing systems*, 29, 2016.

Michaël Defferrard, Lionel Martin, Rodrigo Pena, and Nathanaël Perraudin. Pygsp: Graph signal processing in python, October 2017. URL https://doi.org/10.5281/zenodo.1003158.

Inderjit S Dhillon, Yuqiang Guan, and Brian Kulis. Weighted graph cuts without eigenvectors a multilevel approach. *IEEE transactions on pattern analysis and machine intelligence*, 29(11): 1944–1957, 2007.

Frederik Diehl. Edge contraction pooling for graph neural networks. *arXiv preprint arXiv:1905.10990*, 2019.

Yushun Dong, Kaize Ding, Brian Jalaian, Shuiwang Ji, and Jundong Li. Adagnn: Graph neural networks with adaptive frequency response filter. In *Proceedings of the 30th ACM international conference on information & knowledge management*, pp. 392–401, 2021.

Alexandre Duval and Fragkiskos Malliaros. Higher-order clustering and pooling for graph neural networks. In *Proceedings of the 31st ACM international conference on information & knowledge management*, pp. 426–435, 2022.

Moshe Eliasof, Lars Ruthotto, and Eran Treister. Improving graph neural networks with learnable propagation operators. In *International Conference on Machine Learning*, pp. 9224–9245. PMLR, 2023.

Federico Errica, Marco Podda, Davide Bacciu, and Alessio Micheli. A fair comparison of graph neural networks for graph classification. In *International Conference on Learning Representations*, 2020.

Matthias Fey and Jan E. Lenssen. Fast graph representation learning with PyTorch Geometric. In *ICLR Workshop on Representation Learning on Graphs and Manifolds*, 2019.

Guoji Fu, Peilin Zhao, and Yatao Bian. p-laplacian based graph neural networks. In *International Conference on Machine Learning*, pp. 6878–6917. PMLR, 2022.

H. Gao, Y. Liu, and S. Ji. Topology-aware graph pooling networks. *IEEE Transactions on Pattern Analysis and Machine Intelligence*, 43(12):4512–4518, dec 2021. ISSN 1939-3539. doi: 10.1109/TPAMI.2021.3062794.

Hongyang Gao and Shuiwang Ji. Graph u-nets. In *international conference on machine learning*, pp. 2083–2092. PMLR, 2019.

Xing Gao, Wenrui Dai, Chenglin Li, Hongkai Xiong, and Pascal Frossard. ipool—information-based pooling in hierarchical graph neural networks. *IEEE Transactions on Neural Networks and Learning Systems*, 33(9):5032–5044, 2022. doi: 10.1109/TNNLS.2021.3067441.

Michel X. Goemans and David P. Williamson. Improved approximation algorithms for maximum cut and satisfiability problems using semidefinite programming. *J. ACM*, 42(6):1115–1145, nov 1995. ISSN 0004-5411. doi: 10.1145/227683.227684.

Daniele Grattarola, Daniele Zambon, Filippo Maria Bianchi, and Cesare Alippi. Understanding pooling in graph neural networks. *IEEE Transactions on Neural Networks and Learning Systems*, 2022.

Jonas Berg Hansen and Filippo Maria Bianchi. Total variation graph neural networks. In *International Conference on Machine Learning*, pp. 12445–12468. PMLR, 2023.

Weihua Hu, Bowen Liu, Joseph Gomes, Marinka Zitnik, Percy Liang, Vijay Pande, and Jure Leskovec. Strategies for pre-training graph neural networks, 2020.

Yu Jin, Andreas Loukas, and Joseph JaJa. Graph coarsening with preserved spectral properties. In *International Conference on Artificial Intelligence and Statistics*, pp. 4452–4462. PMLR, 2020.

Amir Hosein Khasahmadi, Kaveh Hassani, Parsa Moradi, Leo Lee, and Quaid Morris. Memory-based graph networks. In *International Conference on Learning Representations*, 2020.

Diederik P. Kingma and Jimmy Ba. Adam: A method for stochastic optimization. In *3rd International Conference on Learning Representations, ICLR 2015, San Diego, CA, USA, May 7-9, 2015, Conference Track Proceedings*, 2015.

Thomas N. Kipf and Max Welling. Semi-supervised classification with graph convolutional networks. In *5th International Conference on Learning Representations, ICLR 2017, Toulon, France, April 24-26, 2017, Conference Track Proceedings*. OpenReview.net, 2017.

Boris Knyazev, Graham W Taylor, and Mohamed Amer. Understanding attention and generalization in graph neural networks. *Advances in neural information processing systems*, 32, 2019.

Francesco Landolfi. Revisiting edge pooling in graph neural networks. In *ESANN*, 2022.

Junhyun Lee, Inyeop Lee, and Jaewoo Kang. Self-attention graph pooling. In *International conference on machine learning*, pp. 3734–3743. PMLR, 2019.

W Bernard Lee and Anthony G Constantinides. Quantumized graph cuts in portfolio construction and asset selection. *Springer-Nature Transactions on Computational Science and Compu-tational Intelligence*, 2023.

Frauke Liers, Michael Jünger, Gerhard Reinelt, and Giovanni Rinaldi. Computing exact ground states of hard ising spin glass problems by branch-and-cut. *New optimization algorithms in physics*, pp. 47–69, 2004.

Derek Lim, Felix Hohne, Xiuyu Li, Sijia Linda Huang, Vaishnavi Gupta, Omkar Bhalerao, and Ser Nam Lim. Large scale learning on non-homophilous graphs: New benchmarks and strong simple methods. *Advances in Neural Information Processing Systems*, 34:20887–20902, 2021.

Ning Liu, Songlei Jian, Dongsheng Li, Yiming Zhang, Zhiquan Lai, and Hongzuo Xu. Hierarchical adaptive pooling by capturing high-order dependency for graph representation learning. *IEEE Transactions on Knowledge and Data Engineering*, 35(4):3952–3965, 2021.

Andreas Loukas. Graph reduction with spectral and cut guarantees. *Journal of Machine Learning Research*, 20(116):1–42, 2019.

Enxhell Luzhnica, Ben Day, and Pietro Lio. Clique pooling for graph classification. *arXiv preprint arXiv:1904.00374*, 2019.

Zheng Ma, Junyu Xuan, Yu Guang Wang, Ming Li, and Pietro Liò. Path integral based convolution and pooling for graph neural networks. *Advances in Neural Information Processing Systems*, 33: 16421–16433, 2020.

Konstantin Makarychev, Yury Makarychev, and Aravindan Vijayaraghavan. Bilu–linial stable instances of max cut and minimum multiway cut. In *Proceedings of the twenty-fifth annual ACM-SIAM symposium on Discrete algorithms*, pp. 890–906. SIAM, 2014.

Ivan Marisca, Cesare Alippi, and Filippo Maria Bianchi. Graph-based forecasting with missing data through spatiotemporal downsampling. In *Proceedings of the 41st International Conference on Machine Learning*, volume 235 of *Proceedings of Machine Learning Research*, pp. 34846–34865. PMLR, 2024.

Paul M Mather and Magaly Koch. *Computer processing of remotely-sensed images*. John Wiley & Sons, 2022.

Christopher Morris, Nils M. Kriege, Franka Bause, Kristian Kersting, Petra Mutzel, and Marion Neumann. Tudataset: A collection of benchmark datasets for learning with graphs. In *ICML 2020 Workshop on Graph Representation Learning and Beyond (GRL+ 2020)*, 2020.

Emmanuel Noutahi, Dominique Beaini, Julien Horwood, Sébastien Giguère, and Prudencio Tossou. Towards interpretable sparse graph representation learning with laplacian pooling. *arXiv preprint arXiv:1905.11577*, 2019.

Yunsheng Pang, Yunxiang Zhao, and Dongsheng Li. Graph pooling via coarsened graph infomax. In *Proceedings of the 44th International ACM SIGIR Conference on Research and Development in Information Retrieval*, pp. 2177–2181, 2021.

Oleg Platonov, Denis Kuznedelev, Michael Diskin, Artem Babenko, and Liudmila Prokhorenkova. A critical look at the evaluation of GNNs under heterophily: Are we really making progress? In *The Eleventh International Conference on Learning Representations*, 2023.

Ekagra Ranjan, Soumya Sanyal, and Partha Talukdar. Asap: Adaptive structure aware pooling for learning hierarchical graph representations. In *Proceedings of the AAAI Conference on Artificial Intelligence*, volume 34, pp. 5470–5477, 2020.

Martin JA Schuetz, J Kyle Brubaker, and Helmut G Katzgraber. Combinatorial optimization with physics-inspired graph neural networks. *Nature Machine Intelligence*, 4(4):367–377, 2022.

David I Shuman, Sunil K. Narang, Pascal Frossard, Antonio Ortega, and Pierre Vandergheynst. The emerging field of signal processing on graphs: Extending high-dimensional data analysis to networks and other irregular domains. *IEEE Signal Processing Magazine*, 30(3):83–98, 2013. doi: 10.1109/MSP.2012.2235192.

David I Shuman, Mohammad Javad Faraji, and Pierre Vandergheynst. A multiscale pyramid transform for graph signals. *IEEE Transactions on Signal Processing*, 64(8):2119–2134, 2015.

Nicolas Tremblay, Paulo Gonçalves, and Pierre Borgnat. Design of graph filters and filterbanks. In *Cooperative and Graph Signal Processing*, pp. 299–324. Elsevier, 2018.

Luca Trevisan. Max cut and the smallest eigenvalue. In *Proceedings of the forty-first annual ACM symposium on Theory of computing*, pp. 263–272, 2009.

Anton Tsitsulin, John Palowitch, Bryan Perozzi, and Emmanuel Müller. Graph clustering with graph neural networks. *J. Mach. Learn. Res.*, 24:127:1–127:21, 2023.

Ulrike von Luxburg. A tutorial on spectral clustering, 2007.

Guangtao Wang, Rex Ying, Jing Huang, and Jure Leskovec. Improving graph attention networks with large margin-based constraints, 2019.

Pengyun Wang, Junyu Luo, Yanxin Shen, Siyu Heng, and Xiao Luo. A comprehensive graph pooling benchmark: Effectiveness, robustness and generalizability. *arXiv preprint arXiv:2406.09031*, 2024.

Felix Wu, Amauri Souza, Tianyi Zhang, Christopher Fifty, Tao Yu, and Kilian Weinberger. Simplifying graph convolutional networks. In Kamalika Chaudhuri and Ruslan Salakhutdinov (eds.), *Proceedings of the 36th International Conference on Machine Learning*, volume 97 of *Proceedings of Machine Learning Research*, pp. 6861–6871. PMLR, 09–15 Jun 2019.

Junran Wu, Xueyuan Chen, Ke Xu, and Shangzhe Li. Structural entropy guided graph hierarchical pooling. In *International conference on machine learning*, pp. 24017–24030. PMLR, 2022.

Keyulu Xu, Weihua Hu, Jure Leskovec, and Stefanie Jegelka. How powerful are graph neural networks? In *International Conference on Learning Representations*, 2019.

Yinyu Ye. The gset dataset, 2003.

Zhitao Ying, Jiaxuan You, Christopher Morris, Xiang Ren, Will Hamilton, and Jure Leskovec. Hierarchical graph representation learning with differentiable pooling. *Advances in neural information processing systems*, 31, 2018.

Hao Yuan and Shuiwang Ji. Structpool: Structured graph pooling via conditional random fields. In *Proceedings of the 8th International Conference on Learning Representations*, 2020.

Zhen Zhang, Jiajun Bu, Martin Ester, Jianfeng Zhang, Chengwei Yao, Zhi Yu, and Can Wang. Hierarchical graph pooling with structure learning. *arXiv preprint arXiv:1911.05954*, 2019.

Jie Zhou, Ganqu Cui, Shengding Hu, Zhengyan Zhang, Cheng Yang, Zhiyuan Liu, Lifeng Wang, Changcheng Li, and Maosong Sun. Graph neural networks: A review of methods and applications. *AI Open*, 1:57–81, 2020a. ISSN 2666-6510. doi: 10.1016/j.aiopen.2021.01.001.

Leo Zhou, Sheng-Tao Wang, Soonwon Choi, Hannes Pichler, and Mikhail D Lukin. Quantum approximate optimization algorithm: Performance, mechanism, and implementation on near-term devices. *Physical Review X*, 10(2):021067, 2020b.

APPENDIX

A NEAREST NEIGHBOR ASSOCIATION ALGORITHM

As discussed in Sec. 3, each node is associated to one of the supernodes (preferably the closest in terms of path-distance on the graph). Naively searching for each node the closest supernode is computationally demanding and becomes intractable for large graphs. Therefore, we propose an implementation of the assignment scheme that is efficient and can be easily parallelized on a GPU. The proposed algorithm is based on a Breadth First Search (BFS) of the graph and is detailed in the pseudo-code in Algorithm 1.

Algorithm 1 Pseudo-code for the assignment scheme to the supernodes

1: **procedure** ASSIGNNODESTOSUPERNODES($\mathcal{G}, \mathcal{S}, MaxIter$)
2: $\boldsymbol{E} \leftarrow$ InitializeEncodings($\mathcal{G}, \mathcal{S}$) ▷ One-hot encoding
3: $\boldsymbol{m} \leftarrow$ InitializeMask($\mathcal{G}, \mathcal{S}$)
4: $Assignments \leftarrow$ InitializeEmptyList()
5: **for** $i = 1$ to $MaxIter$ **do**
6: **if** AllNodesAssigned($\boldsymbol{m}$) **then**
7: **break**
8: **end if**
9: $\boldsymbol{E}' \leftarrow$ ParallelMessagePassing($\mathcal{G}, \boldsymbol{E}$) ▷ $\boldsymbol{E}' = \boldsymbol{A}\boldsymbol{E}$
10: $Assignments \leftarrow$ ParallelAssignment($\boldsymbol{E}', \mathcal{S}, \boldsymbol{m}$)
11: $\boldsymbol{m} \leftarrow$ UpdateMask($\boldsymbol{m}, Assignments$)
12: $\boldsymbol{E} \leftarrow \boldsymbol{E}'$
13: **end for**
14: **if** not AllNodesAssigned($\boldsymbol{m}$) **then**
15: $RndAssignments \leftarrow$ ParallelRandomAssignment($UnassignedNodes, \mathcal{S}$)
16: **end if**
17: $FinalAssignments \leftarrow$ GetFinalAssignments($Assignments, RndAssignments$)
18: **return** $FinalAssignments$
19: **end procedure**

The algorithm takes as input the graph $\mathcal{G}$ (in particular, its topology described by the adjacency matrix $\boldsymbol{A}$), the set of K supernodes $\mathcal{S}$ identified by the `SEL` operation, and a maximum number of iterations ($MaxIter$), which represent the maximum number of steps a node can traverse the graph to reach its closest supernode before being assigned at random.

In line 2, an encoding matrix $\boldsymbol{E}$ of size $N \times K + 1$ is initialized so that row i is a one-hot vector with the non-zero entry in position $k + 1$, if the node i of the original graph is the k-th supernode. Otherwise, row i in a zero-vector of size $K + 1$. This matrix will be gradually populated when supernodes are encountered during the BFS. It's important to note that the 0-th column in matrix $\boldsymbol{E}$ (and subsequently in $\boldsymbol{E}'$) serves a special purpose. This column represents a "fake" supernode, which plays a crucial role in the assignment process.

A Boolean mask $\boldsymbol{m} \in \{0, 1\}^N$ indicating whether a node already encountered the closest supernode is initialized in line 3 with 1 in position i is nodes i is a supernode and 0 otherwise. Finally, an empty list indicating to which supernode each node is assigned is initialized (line 4).

Until the maximum number of iterations is reached or until all nodes are assigned (line 6), the encoding matrix $\boldsymbol{E}$ is propagated with an efficient message passing operation (line 9) that can be parallelized on a GPU. As soon as a 1 appears in position k within a line i of $\boldsymbol{E}$ previously full of zeros, node i is assigned to supernode k and the assignments and mask $\boldsymbol{m}$ are updated accordingly (lines 10 and 11). The *ParallelAssignment* function (line 10), in particular, takes the rows of the newly generated embeddings $\boldsymbol{E}'$ that have not yet been assigned and performs an `argmax` operation on the last dimension. If the `argmax` doesn't find any valid supernode for a node (*i.e.*, all values in the row are zero), it returns 0, effectively assigning the node to the "fake" supernode represented by the 0-th column. This allows to filter out the unassigned nodes in line 11.

If there are still unassigned nodes at the end of the iterations, the remaining nodes are randomly assigned to one of the K supernodes (line 15). Finally, all the assignments are merged (line 17).

B DERIVATION OF THE AUXILIARY LOSS

Let us consider the MAXCUT objective in Equation 1. It can be rewritten as

$$\max_{\boldsymbol{z}} \left(\sum_{i,j \in \mathcal{V}} w_{ij} - \sum_{i,j \in \mathcal{V}} z_i z_j w_{ij} \right) = \max_{\boldsymbol{z}} \left(|E| - \sum_{i,j \in \mathcal{V}} z_i z_j w_{ij} \right),$$

which is equivalent to

$$\max_{\boldsymbol{z}} \left(1 - \sum_{i,j \in \mathcal{V}} \frac{z_i z_j w_{ij}}{|E|} \right).$$

The solution $\boldsymbol{z}^*$ for the original objective is thus the solution for

$$\min_{\boldsymbol{z}} \frac{\boldsymbol{z}^\top A \boldsymbol{z}}{|E|}.$$

C IMPLEMENTATION DETAILS

C.1 MAXCUTPOOL LAYER AND SCORENET

A schematic depiction of the MaxCutPool layer is illustrated in Fig. 3, where the SEL, RED, and CON operations are highlighted.

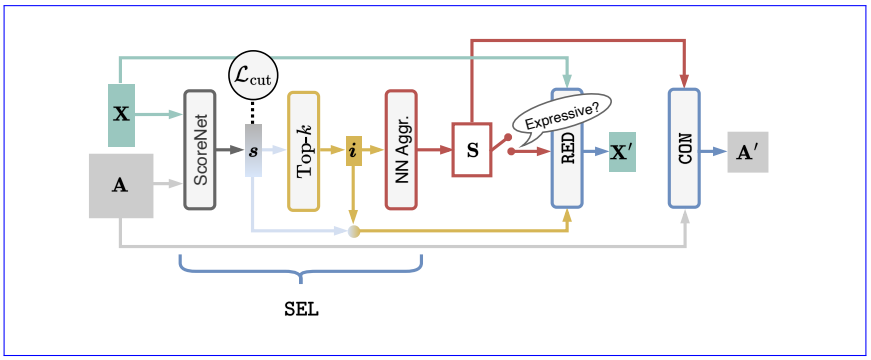

Figure 3: Scheme of the MaxCutPool layer.

SEL first computes a score vector $\boldsymbol{s}$ using the auxiliary GNN, ScoreNet, based on the node features $\mathbf{X}$ and the connectivity matrix $\mathbf{A}$. A top-K operation is used to find the indices $\boldsymbol{i}$ of the K nodes with the highest scores that become the supernodes, *i.e.*, the nodes of the pooled graph. The remaining $N - K$ nodes are assigned to the nearest supernode through a nearest-neighbor (NN) aggregation procedure that yields an assignment matrix $\mathbf{S}$, whose jk-th element is 1 if nodes j is assigned to supernode k, and zero otherwise. The score vector $\boldsymbol{s}$ is used to compute the loss $\mathcal{L}_{\text{cut}}$, which is associated with each MaxCutPool layer.

The RED operation computes the node features of the pooled graph $\boldsymbol{X}'$ by multiplying the features of the selected nodes $\boldsymbol{X}_i$ with the scores $\boldsymbol{s}$. This operation is necessary to let the gradients flow past the top-K operation, which is not differentiable. In the expressive variant, MaxCutPool-E, RED computes the new node features by combining those from all the nodes in the graph through the multiplication with matrix $\boldsymbol{S}$. We combine the features by summing them instead of taking the average since the sum enhances the expressiveness of the pooling layer (Bianchi & Lachi, 2023).

The CON operations always leverage the assignment matrix to compute the adjacency matrix of the pooled graph. In particular, the edge connecting two supernodes i and j is obtained by coalescing all the edges connecting the nodes assigned to supernode i with those assigned to supernode j. Also in this case, we take the sum as the operation to coalesce the edges. The resulting edges in the pooled graph are associated with a weight w_{ij} that counts the number of combined edges.

The details of the ScoreNet used in the MaxCutPool layer are depicted in Fig. 4. The ScoreNet consists of a linear layer that maps the features $\boldsymbol{X}$ to a desired hidden dimension. Afterward, a stack of HetMP layers gradually transforms the node features by amplifying their high-frequency components with heterogeneous MP operations. Finally, an MLP transforms the node features of the last HetMP layer into score vector $\boldsymbol{s}$, which is a high-frequency graph signal. We note that while the

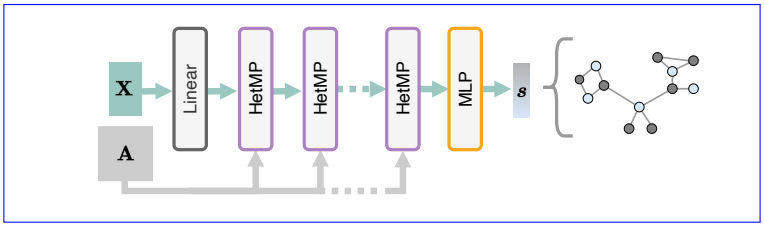

Figure 4: Scheme of the ScoreNet.

simple HetMP we adopted works well in our case, different heterophilic MP operators could have been considered (Chien et al., 2021; Dong et al., 2021; Fu et al., 2022).

The ScoreNet is configured with the following hyperparameters:

- Number of HetMP layers and number of features in each layer. We use the notation $[32, 16, 8]$ to indicate a ScoreNet with three HetMP layers with hidden sizes 32, 16, and 8, respectively. We also use the notation $[32] \times 4$ to indicate 4 layers with 32 units each. As default, we use $[32, 32, 32, 32, 16, 16, 16, 16, 8, 8, 8, 8]$.
- Activation function of the HetMP layers. As default, we use TanH.
- Number of layers and features in the MLP. As default, we use $[16, 16]$.
- Activation function of the MLP. As default, we use ReLU.
- Smoothness hyperparameter δ. As default, we use 2.
- Auxiliary loss weight β. As default, we use 1.

The optimal configuration has been identified with the cross-validation procedure described in Sec.4. Depending on the experiment and the GNN architecture, some parameters in the ScoreNet are kept fixed at their default value while others are optimized.

C.2 CUT MODEL

The model used to compute the MAXCUT is depicted in Fig. 5. The model consists of a single MP layer followed by the ScoreNet, which returns the score vector $\boldsymbol{s}$. The MAXCUT partition is obtained

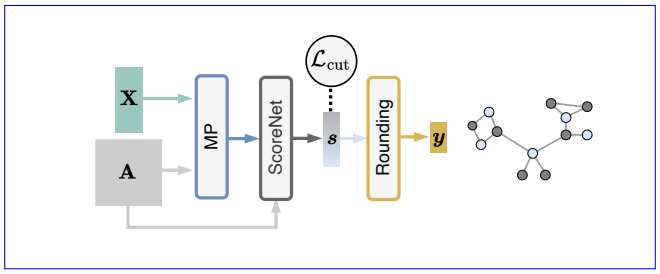

Figure 5: Scheme of the model used for computing the MAXCUT.

by rounding the values in the score vector as follows

$$y_i = \begin{cases} 1 & \text{if } s_i > 0, \\ -1 & \text{otherwise.} \end{cases}$$

The model is trained in a completely unsupervised fashion only by minimizing the auxiliary loss $\mathcal{L}_{\text{cut}}$.

As MP layers we used a GIN (Xu et al., 2019) layer with 32 units and ELU activation function. The model was trained for 2000 epochs with Adam optimizer (Kingma & Ba, 2015), with the initial learning rate set to $8e-4$. We used a learning rate scheduler that reduces by 0.8 the learning rate when the auxiliary loss does not improve for 100 epochs. For testing, we restored the model checkpoint that achieved the lowest auxiliary loss.

The best configuration was found via a grid search on the following set of hyperparameters:

- HetMP layers and units:
  - $[32] \times 4$,
  - $[4] \times 32$,
  - $[8] \times 16$,
  - $[16] \times 8$,
  - $[32, 32, 32, 32, 16, 16, 16, 16, 8, 8, 8, 8]$.
- HetMP activations:
  - ReLU,
  - TanH.
- Smoothness hyperparameter δ:
  - 2,
  - 3,
  - 5.

In Tab. 5 we report the configurations of the ScoreNet used for the different graphs in the `MAXCUT` experiment.

Table 5: Hyperparameters configurations of the ScoreNet for the `MAXCUT` task.

Dataset	MP units	MP Act	δ
G14	$[32, 32, 32, 32, 16, 16, 16, 16, 8, 8, 8, 8]$	ReLU	2.0
G15	$[32, 32, 32, 32, 16, 16, 16, 16, 8, 8, 8, 8]$	ReLU	2.0
G22	$[4] \times 32$	TanH	2.0
G49	$[32, 32, 32, 32, 16, 16, 16, 16, 8, 8, 8, 8]$	TanH	2.0
G50	$[8] \times 16$	ReLU	2.0
G55	$[4] \times 32$	ReLU	2.0
G70	$[8] \times 16$	ReLU	2.0
BarabasiAlbert	$[4] \times 32$	TanH	2.0
Community	$[4] \times 32$	TanH	2.0
ErdősRenyi	$[4] \times 32$	TanH	2.0
Grid2d (10×10)	$[4] \times 32$	TanH	2.0
Grid2d (60×40)	$[4] \times 32$	ReLU	2.0
Minnesota	$[4] \times 32$	TanH	2.0
RandRegular	$[4] \times 32$	TanH	2.0
Ring	$[4] \times 32$	ReLU	2.0
Sensor	$[4] \times 32$	TanH	2.0

C.3 Graph classification model

The model used to perform graph classification is depicted in Fig. 6. The model consists of an MP layer, followed by a pooling layer, an MP acting on the pooled graph, a global pooling layer that sums

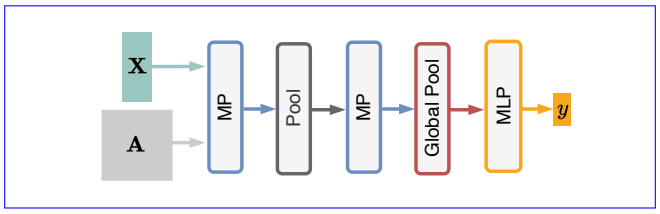

Figure 6: Scheme of the graph classification model.

the features of all the nodes in the pooled graph, and an MLP that produces the label y associated with the input graph. The model is trained by jointly minimizing the cross-entropy loss between the predicted graph labels and the true ones and the auxiliary losses associated with the different pooling layers. The models are trained using a batch size of 32 for 1000 epochs, using the Adam optimizer with an initial learning rate of $1e-4$. We used an early stopping that monitors the validation loss with a patience of 300 epochs. For testing, we restored the model checkpoint that achieved the lowest validation loss during training.

The best configuration was found via a grid search on the following set of hyperparameters:

- HetMP layers and units:
  - $[32] \times 8$,
  - $[32] \times 4$,
  - $[8] \times 16$, $[16] \times 8$,
  - $[32, 32, 16, 16, 8, 8]$,
  - $[32, 32, 32, 32, 16, 16, 16, 16, 8, 8, 8, 8]$.
- Auxiliary loss weight β:
  - 1,
  - 2,
  - 5.

Table 6: Hyperparameters configurations of the ScoreNet for the graph classification task.

	MaxCutPool		**MaxCutPool-E**	
Dataset	**MP units**	$\boldsymbol{\beta}$	**MP units**	$\boldsymbol{\beta}$
GCB-H	$[8] \times 16$	3.0	$[32] \times 8$	5.0
COLLAB	$[32] \times 8$	1.0	$[32] \times 8$	1.0
DD	$[32, 32, 32, 32, 16, 16, 16, 16, 8, 8, 8, 8]$	1.0	$[8] \times 16$	5.0
ENZYMES	$[8] \times 16$	3.0	$[16] \times 8$	3.0
EXPWL1	$[32, 32, 16, 16, 8, 8]$	1.0	$[16] \times 8$	1.0
MUTAG	$[8] \times 16$	1.0	$[16] \times 8$	3.0
Multipartite	$[32] \times 8$	3.0	$[32] \times 8$	1.0
Mutagenicity	$[32, 32, 16, 16, 8, 8]$	1.0	$[32] \times 8$	5.0
NCI1	$[32, 32, 16, 16, 8, 8]$	1.0	$[8] \times 16$	3.0
PROTEINS	$[32, 32, 32, 32, 16, 16, 16, 16, 8, 8, 8, 8]$	3.0	$[32, 32, 16, 16, 8, 8]$	5.0
REDDIT-B	$[32] \times 8$	1.0	$[32, 32, 32, 32, 16, 16, 16, 16, 8, 8, 8, 8]$	1.0

In Tab. 6 we report the configurations of the ScoreNet used in the graph classification architecture for the different datasets in the expressive and non-expressive variant of MaxCutPool.

C.4 Node classification model

The model used to perform node classification is depicted in Fig. 7. The model consists of an MP layer, followed by a pooling layer, an MP acting on the pooled graph, an unpooling (lifting) layer, an MP on the unpooled graph, and an MLP that produces the final node labels $\boldsymbol{y}$.

The entry y_i represents the predicted label for node i. The model is trained by jointly minimizing the cross-entropy loss between the predicted node labels and the true ones and the auxiliary loss of the pooling layer.

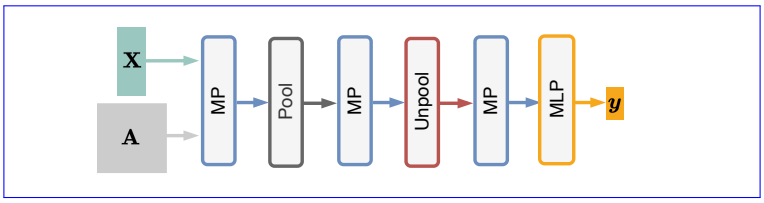

Figure 7: Scheme of the node classification model.

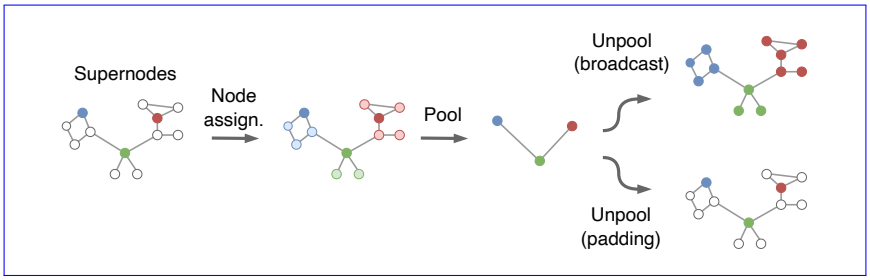

Figure 8: The two possible strategies for performing unpooling (lifting).

When using MaxCutPool, the unpooling/lifting procedure can be implemented in two different ways, illustrated in Fig. 8. The first strategy, *broadcast* unpooling, copies the values $\boldsymbol{X}'$ of the nodes of the pooled graph to both the corresponding supernodes and to the nodes associated with the supernodes according to the assignment matrix $\boldsymbol{S}$, obtained as described in Sec. 3 and Appendix A. Formally, the unpooled node features $\tilde{\boldsymbol{X}}$ are:

$$\tilde{\boldsymbol{X}} = \boldsymbol{S}\boldsymbol{X}'.$$

We note that this is the commonly used approach to perform unpooling in cluster-based poolers.

In the second strategy, *padding* unpooling, the values $\boldsymbol{X}'$ are copied back only to the supernodes, while the remaining nodes are padded with a zero-valued vector:

$$[\tilde{\boldsymbol{X}}]_i = \begin{cases} [\boldsymbol{X}']_i & \text{if } i \text{ is a supernode} \\ \boldsymbol{0} & \text{otherwise.} \end{cases}$$

This is the approach to perform unpooling used by scoring-based approaches such as Top-k and by one-over-K approaches such as NDP that only select the supernodes and leave the remaining nodes unassigned.

For the node classification task presented in Sec. 4.3, as MP layers we used a GIN (Xu et al., 2019) layer with 32 units and ReLU activation function. The MLP has a single hidden layer with 32 units, a ReLU activation function, and a dropout layer between the hidden and output layers with a dropout probability of 0.1. The unpooling strategy used in this architecture is the broadcast one for k-MIS and MaxCutPool and the padding one for Top-k and NDP.

The best configuration was found via a grid search on the following set of hyperparameters:

- HetMP layers and units:
  - $[32] \times 4$,
  - $[4] \times 32$,
  - $[32, 32, 32, 32, 16, 16, 16, 16, 8, 8, 8, 8]$.
- MLP activations:
  - ReLU,
  - TanH.

The configuration of the ScoreNet for the MaxCutPool pooler used in the different datasets is reported in Tab. 7.

Table 7: Hyperparameters configurations of the ScoreNet in the node classification task.

Dataset	MP units	MLP Act.
Roman-Empire	$[32, 32, 32, 32]$	ReLU
Amazon-Ratings	$[32, 32, 32, 32]$	ReLU
Minesweeper	$[32, 32, 32, 32, 16, 16, 16, 16, 8, 8, 8, 8]$	ReLU
Tolokers	$[32, 32, 32, 32, 16, 16, 16, 16, 8, 8, 8, 8]$	ReLU
Questions	$[32, 32, 32, 32]$	ReLU

The node classifier was trained for $20,000$ epochs, using the Adam optimizer with an initial learning rate of $5e-4$. We used a learning rate scheduler that reduces by 0.5 the learning rate when the validation loss does not improve for 500 epochs. We used an early stopping that monitors the validation loss with a patience of $2,000$ epochs. For testing, we restored the model checkpoint that achieved the lowest validation loss during training.

We considered also an additional architecture for node classification with skip (residual) connections, depicted in Fig. 9. This architecture is similar to the Graph U-Net proposed by Gao & Ji (2019). The

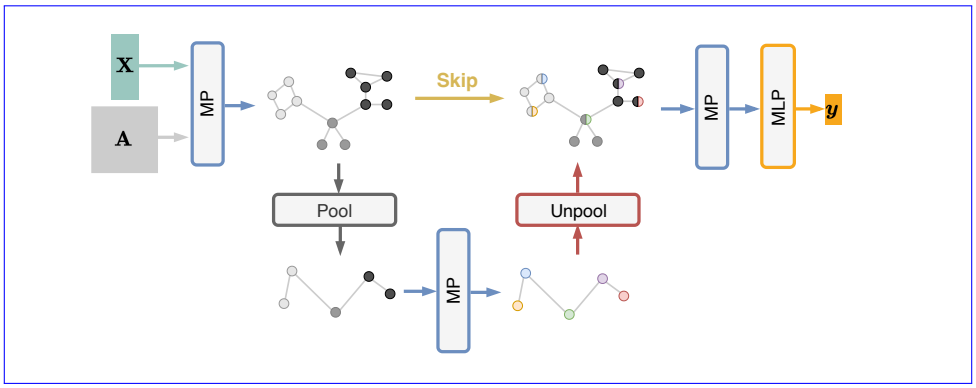

Figure 9: Scheme of the node classification model with skip connections.

node features obtained after the first MP layer are concatenated to the node features generated by the unpooling step. In this architecture, we used the broadcast unpooling for k-MIS and padding unpooling for MaxCutPool, Top-k, and NDP. The results obtained with this architecture are reported in App. E. In Tab. 8 we report the configurations of the ScoreNet used in the architecture with skip connection in the different datasets.

Table 8: Hyperparameters configurations for the node classification task based on the architecture with skip connections.

Dataset	**MP units**	**MLP Act.**
Roman-Empire	[32, 32, 32, 32]	ReLU
Amazon-Ratings	[32, 32, 32, 32]	ReLU
Minesweeper	[32, 32, 32, 32]	TanH
Tolokers	[32, 32, 32, 32]	ReLU
Questions	[32, 32, 32, 32]	ReLU

C.5 IMPLEMENTATION OF OTHER POOLING LAYERS

The pooling methods Top-k, Diffpool, DMoN, Graclus, and MinCutPool are taken from PyTorch Geometric (Fey & Lenssen, 2019). For k-MIS we used the official implementation [2]. For ECPool, we used the efficient parallel implementation [3] proposed by Landolfi (2022). For NDP we adapted to PyTorch the original Tensorflow implementation [4]. All pooling layers were used with the default hyperparameters. Since k-MIS does not allow to directly specify the pooling ratio, we set $k = \lfloor 1/k \rfloor$.

D DATASETS DETAILS

D.1 CUT DATASETS

The statistics of the PyGSP and the Gset datasets used to compute the MAXCUT partition in Sec. 4.1 are reported in Tab. 9. While the PyGSP graphs are built from the library (Defferrard et al., 2017), the Gset dataset is downloaded from the original source [5].

Table 9: Statistics of the PyGSP datasets used to compute the MAXCUT.

(a) PyGSP datasets

Dataset	# Nodes	# Edges	Vertex attr.
Barabasi-Albert	100	768	2
Community	90	532	2
Erdős-Renyi	100	974	2
Grid2d (10×10)	100	360	2
Grid2d (60×40)	2,400	9400	2
Minnesota	2642	6608	2
RandRegular	500	1500	2
Ring	100	200	2
Sensor	64	640	2

(b) Gset

Dataset	# Nodes	# Edges	Vertex attr.
G14	800	$4,694$	–
G15	800	$4,661$	–
G22	$2,000$	$19,990$	–
G49	$3,000$	$6,000$	–
G50	$3,000$	$6,000$	–
G55	$5,000$	$12,468$	–
G70	$10,000$	$9,999$	–

D.2 MULTIPARTITE DATASET DESCRIPTION

The Multipartite graph dataset is a synthetic dataset consisting of complete multipartite graphs. The nodes of each graph can be partitioned into C clusters of independent nodes, such that every node is connected to every node belonging to every other cluster. The generation of the graphs and the class labels is formally described by the pseudo-code in Algorithm 2 and is discussed in the following.

1. A set of C cluster centers with 2D coordinates (x, y) is initially arranged in a polygon shape. Each center is associated with a label, *i.e.*, a color.
2. The graph class is determined by the position and the color of the cluster centers. Specifically, the graph class is given by the color of the cluster whose center is on the positive x-axis.
3. For each class, we generate multiple graphs using these cluster centers. A graph is created by drawing at random the position of the nodes around each cluster center. The number of nodes per cluster varies randomly up to a maximum. Nodes within a cluster share the same color, which is determined by the cluster center.
4. The topology of each graph is obtained by connecting nodes from one cluster to the nodes of all the other clusters, but not to the nodes of the same cluster. Therefore, a node is connected only to nodes with different colors, making the graphs highly heterophilic.
5. After generating graphs for one class, the cluster centers are rotated, and this rotated configuration is used for the next class. Indeed, each rotation brings a different cluster to the positive x-axis.

[2] https://github.com/flandolfi/k-mis-pool
[3] https://github.com/flandolfi/edge-pool
[4] https://github.com/danielegrattarola/decimation-pooling
[5] http://web.stanford.edu/~yyye/yyye/Gset/

Algorithm 2 Multipartite graph dataset generation

Input: num_clusters, max_nodes_per_cluster, graphs_per_class
Output: dataset

```
cluster_centers ← GeneratePolygonVertices(num_clusters)          ▷ Initial arrangement of centers
dataset ← {}
for class_label ← 0 to num_clusters - 1 do
    for 1 to graphs_per_class do
        graph ← GenerateMultipartiteGraph(cluster_centers, max_nodes_per_cluster)
        graph.label ← class_label                                ▷ Label based on current rotation
        Add graph to dataset
    end for
    cluster_centers ← RotateClockwise(cluster_centers)           ▷ Rotate for next class
end for
return dataset

function GenerateMultipartiteGraph(cluster_centers, max_nodes_per_cluster)
    for each center in cluster_centers do
        num_nodes ← RandomInt(1, max_nodes_per_cluster)
        node_positions ← GenerateNodesAroundCenter(center, num_nodes)
        node_color ← GetColorForCluster(center)                  ▷ Each cluster has a unique color
        AddNodesToGraph(node_positions, node_color)
    end for
    ConnectNodesAcrossClusters()                                 ▷ Create complete multipartite graph
    return graph
end function

function RotateClockwise(centers)
    return [centers[-1]] + centers[:-1]                          ▷ Move last center to front
end function
```

6. The rotation process continues until the graphs for all the C different classes, whose number is equal to the number of clusters, are generated.

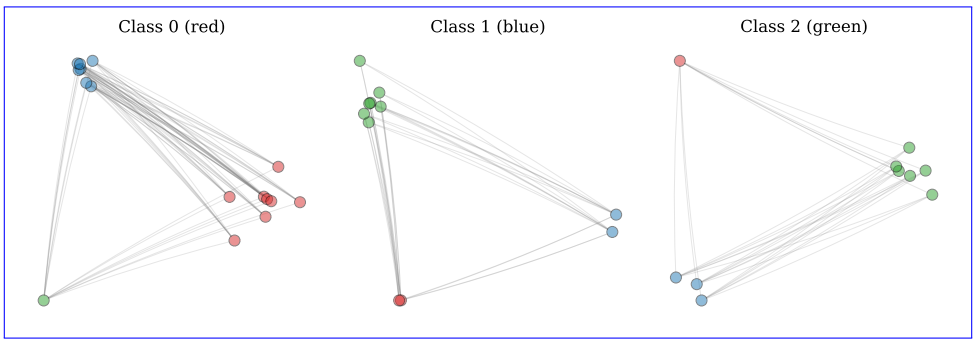

Figure 10: Example of multipartite graphs with $C = 3$ cluster centers generated via our procedure. The graph class corresponds to the color of the nodes from the group to the right.

Examples of multipartite graphs obtained for $C = 3$ are shown in Figure 10.

The process depends on a few parameters that determine the number of clusters, the maximum nodes per cluster, and the number of graphs per class, providing control over the dataset size and complexity. The specific instance of the dataset used in our experiments has 10 centers, 500 graphs per center, and a maximum of 20 nodes per cluster, and is available online [6].

The Multipartite dataset is intentionally designed so that the class label is determined solely by node features: specifically, the color and one of the 2D coordinates (the node's position along the x-axis). Although the graph's topology is structured to ensure that each graph is multipartite, this

[6] hidden_for_peer_review

structure is independent of the class label. This creates an intriguing dichotomy between the graph's topology and its classification labels. In theory, a simple MLP focusing exclusively on node features could accurately solve the classification task, as the graph's topology is essentially irrelevant for determining the correct labels. However, when processed by GNNs, this dataset allows us to explore whether the model can correctly identify and utilize the relevant node features for classification, despite the presence of potentially misleading or noisy topological information. Through this carefully constructed dataset, we aim to highlight the strengths and potential limitations of certain GNNs architectures, particularly in scenarios where the relationship between graph structure and classification labels is non-trivial, such as in heterophilic datasets.

D.3 Graph classification datasets

In addition to the novel Multipartite dataset introduced in Sec. D.2, we consider 10 additional datasets for graph classification in our experimental evaluation. The TU Datasets (Morris et al., 2020) (NCI, PROTEINS, Mutagenicity, COLLAB, REDDIT-B, DD, MUTAG, and Enzymes) are obtained through the loader of PyTorch Geometric [7]. The EXPWL1 and GCB-H datasets, respectively introduced by Bianchi & Lachi (2023) and by Bianchi et al. (2022), are taken from the official repositories [8] [9]. The statistics of each dataset are reported in Tab. 10.

Table 10: Details of the graph classification datasets.

Dataset	#Samples	#Classes	Avg. #vert.	Avg. #edg.	V. attr.	V. lab.	$\bar{h}(\mathcal{D})$
EXPWL1	3,000	2	76.96	186.46	–	yes	0.2740
NCI1	4,110	2	29.87	64.60	–	yes	0.6245
PROTEINS	1,113	2	39.06	72.82	1	yes	0.6582
Mutagenicity	4,337	2	30.32	61.54	–	yes	0.3679
COLLAB	5,000	3	74.49	4,914.43	–	no	1
REDDIT-B	2,000	2	429.63	995.51	–	no	1
GCB-H	1,800	3	148.32	572.32	–	yes	0.8440
DD	1,178	2	284.32	1,431.32	–	yes	0.0688
MUTAG	188	2	17.93	19.79	–	yes	0.7082
ENZYMES	600	6	32.63	62.14	18	yes	0.6687
Multipartite	5000	10	99.79	4,477.43	3	yes	0.1101

Since the node labels are not available in the graph classification setting, it is not possible to rely on the homophily ratio $h(\mathcal{G})$ (Lim et al., 2021) considered in the node classification setting. Therefore, to quantify the degree of homophily in the graphs we look at the node features instead and introduce a surrogate homophily score $\bar{h}(\mathcal{D})$, where $\mathcal{D}$ denotes the whole dataset. The new score is defined as the absolute value of the average cosine similarity between the node features of connected nodes in each graph of the dataset:

$$\bar{h}(\mathcal{D}) = \left| \frac{1}{|\mathcal{D}|} \sum_{\mathcal{G} \in \mathcal{D}} \frac{1}{|\mathcal{E}_{\mathcal{G}}|} \sum_{(i,j) \in \mathcal{E}_{\mathcal{G}}} \frac{\boldsymbol{x}_i \boldsymbol{x}_j}{\|\boldsymbol{x}_i\| \|\boldsymbol{x}_j\|} \right|$$

where $|\mathcal{D}|$ is the number of graphs in the dataset, $\mathcal{E}_{\mathcal{G}}$ is the set of edges of the graph $\mathcal{G}$ and $\boldsymbol{x}_i, \boldsymbol{x}_j$ are the feature vectors of the i-th and j-th node respectively.

D.4 Node classification datasets

The datasets are the heterophilic graphs introduced by Platonov et al. (2023) and are loaded with the API provided by PyTorch Geometric [10]. The nodes of each graph are already split in train, validation, and test across 10 different folds. The statistics of the five datasets are reported in Tab. 11. The

[7] https://pytorch-geometric.readthedocs.io/en/latest/generated/torch_geometric.datasets.TUDataset.html

[8] https://github.com/FilippoMB/The-expressive-power-of-pooling-in-GNNs

[9] https://github.com/FilippoMB/Benchmark_dataset_for_graph_classification

[10] https://pytorch-geometric.readthedocs.io/en/latest/generated/torch_geometric.datasets.HeterophilousGraphDataset.html

Table 11: Statistics of node classification datasets.

Dataset	# Nodes	# Edges	# Classes	$h(\mathcal{G})$
Roman-Empire	22,662	32,927	18	0.021
Amazon-Ratings	24,492	93,050	5	0.127
Minesweeper	10,000	39,402	2	0.009
Tolokers	11,758	519,000	2	0.180
Questions	48,921	153,540	2	0.079

column $h(\mathcal{G})$ is the class insensitive edge homophily ratio as defied by Lim et al. (2021), which represents a measure for the level of homophily in the graph.

E ADDITIONAL RESULTS

E.1 GRAPH CLASSIFICATION

In Tab. 12 we report the additional graph classification results for the dataset where GNNs equipped with different pooling operators did not achieve a significantly different performance from each other.

Table 12: Graph classification accuracy values (subset)

Pooler	DD	MUTAG	ENZYMES	PROTEINS
No pool	$73_{\pm 5}$	$78_{\pm 13}$	$33_{\pm 6}$	$71_{\pm 4}$
Diffpool	$77_{\pm 4}$	$81_{\pm 11}$	$36_{\pm 7}$	$75_{\pm 3}$
DMoN	$78_{\pm 5}$	$82_{\pm 11}$	$37_{\pm 7}$	$76_{\pm 4}$
ECPool	$73_{\pm 5}$	$84_{\pm 12}$	$35_{\pm 8}$	$74_{\pm 5}$
Graclus	$73_{\pm 4}$	$82_{\pm 12}$	$33_{\pm 7}$	$73_{\pm 4}$
k-MIS	$75_{\pm 3}$	$83_{\pm 10}$	$33_{\pm 8}$	$73_{\pm 5}$
MinCutPool	$78_{\pm 5}$	$81_{\pm 12}$	$34_{\pm 9}$	$77_{\pm 5}$
Top-k	$72_{\pm 5}$	$82_{\pm 10}$	$29_{\pm 7}$	$74_{\pm 5}$
MaxCutPool	$77_{\pm 4}$	$84_{\pm 10}$	$31_{\pm 6}$	$74_{\pm 4}$
MaxCutPool-E	$77_{\pm 3}$	$85_{\pm 9}$	$34_{\pm 5}$	$74_{\pm 4}$
MaxCutPool-NL	$74_{\pm 4}$	$83_{\pm 11}$	$31_{\pm 4}$	$70_{\pm 4}$

E.2 NODE CLASSIFICATION

Tab. 13 presents the results for node classification using the architecture with skip connections described in Appendix C.4. For this architecture, we focused on the non-expressive variant of MaxCutPool, which consistently delivered superior performance in this context. The improved results can be attributed to the architecture's ability to preserve the original node information through skip connections. Additionally, by avoiding the combination of neighboring node features (as is done in the expressive variant) the model is better equipped to learn high-frequency features, which is particularly advantageous for heterophilic datasets. For the Minesweeper dataset, we chose to use

Table 13: Node classification accuracy (Roman-empire, Amazon-ratings) and AUROC (Minesweeper, Tolokers, Questions) obtained when using the architecture with skip connections.

Pooler	Roman-e.	Amazon-r.	Minesw.*	Tolokers	Questions	Score
Top-k	$20_{\pm 11}$	$49_{\pm 7}$	$91_{\pm 1}$	$96_{\pm 0}$	$70_{\pm 3}$	1
k-MIS	$19_{\pm 2}$	$53_{\pm 3}$	$90_{\pm 0}$	$91_{\pm 2}$	$82_{\pm 4}$	2
NDP	$19_{\pm 4}$	$56_{\pm 5}$	$94_{\pm 0}$	$90_{\pm 8}$	$69_{\pm 7}$	2
MaxCutPool	$67_{\pm 2}$	$53_{\pm 1}$	$92_{\pm 1}$	$96_{\pm 1}$	$82_{\pm 2}$	**3**

a GIN layer with 16 units as the MP layer, instead of the usual 32 units. This decision was made

because, regardless of the pooling method used, the architecture with skip connections consistently achieved nearly 100% ROC AUC whenever configured with a higher capacity.

F COMPLEXITY

We first discuss the algorithmic complexities and then report empirical measurements about processing time and memory usage. All measurements are done on an Nvidia RTX A6000.

F.1 ALGORITHMIC COMPLEXITY

The complexity of MaxCutPool depends on the complexities of the operations `SEL`, `RED`, and `CON` and of the auxiliary loss $\mathcal{L}_{\text{cut}}$.

`SEL` The complexity of the `SEL` operation depends on the ScoreNet, which consists of a stack of L HetMP layers followed by an MLP, and on the top$_K$ selection.

- **HetMP.** Following the analysis in Blakely et al. (2021), for a graph with N nodes, E edges, and F features, each HetMP layer has a time complexity of $\mathcal{O}(NF^2 + EF)$ and a space complexity of $\mathcal{O}(E + NF + F^2)$. This results in a space and time complexity of $\mathcal{O}(N + E)$ with respect to the input.
- **MLP.** The MLP has a fixed structure with predetermined layer sizes. Since it operates independently on each node's feature vector and the number of operations per node is constant, processing each node takes $\mathcal{O}(1)$ time. With N nodes to process, this results in a total time complexity of $\mathcal{O}(N)$ with respect to the input. The space complexity is also $\mathcal{O}(N)$, as we need to store the MLP hidden and output features for each node.
- **top$_K$** The complexity of sorting an array of N elements is $\mathcal{O}(N \log(N))$. However, if we are interested in finding only the top-K elements the complexity can be lowered to $\mathcal{O}(N \log(K))$ or $\mathcal{O}(N + K)$, depending on the algorithm adopted. Therefore, we can assume an almost-linear complexity in time and space with respect to the number of nodes N.

`RED` For the non-expressive variant, `RED` involves a Hadamard product between the scores and features of the K selected nodes, giving a time complexity of $\mathcal{O}(K)$. The expressive variant requires an additional multiplication with the assignment matrix $\boldsymbol{S}$, increasing the complexity to $\mathcal{O}(K + NF)$. When K is a function of N (e.g., $K = N/2$), both variants have a time complexity of $\mathcal{O}(N)$ with respect to the input.

The space complexity is $\mathcal{O}(N)$, representing the storage of input and output data.

`CON` Our efficient implementation of the nearest neighbor assignment follows the complexity of BFS: $\mathcal{O}(N + E)$ time and $\mathcal{O}(N)$ space.

Auxiliary loss The auxiliary loss $\mathcal{L}_{\text{cut}}$ requires computing a quadratic form, with time complexity $\mathcal{O}(E)$ and space complexity $\mathcal{O}(N + E)$.

Total complexity The overall complexity of MaxCutPool is:

$$\begin{aligned} \text{Time complexity:} \quad & \mathcal{O}(E + N) \\ \text{Space complexity:} \quad & \mathcal{O}(E + N) \end{aligned} \tag{7}$$

These sub-quadratic complexities match those of the most efficient MP and trainable pooling operators.

F.2 EXECUTION TIMES

In Tab. 14 we report the number of seconds used by the architecture for node classification to process a batch when configured with different pooling operators.

Table 14: Execution times in terms of batches processed per second (b/s) by the architecture for node classification configured with different pooling methods.

Pooler	Roman-e.	Amazon-r.	Minesw.	Tolokers	Questions
Diffpool	0.72 b/s	0.93 b/s	0.05 b/s	0.11 b/s	OOM
DMoN	0.66 b/s	0.83 b/s	0.06 b/s	0.11 b/s	OOM
MinCutPool	1.32 b/s	1.63 b/s	0.14 b/s	0.23 b/s	OOM
~~Top-k~~	~~0.01 b/s~~	~~0.01 b/s~~	~~0.01 b/s~~	~~0.01 b/s~~	~~0.03 b/s~~
Graclus	0.01 b/s	0.01 b/s	0.01 b/s	0.01 b/s	0.01 b/s
k-MIS	0.01 b/s	0.01 b/s	0.04 b/s	0.01 b/s	0.01 b/s
NDP	0.01 b/s	0.01 b/s	0.00 b/s	0.01 b/s	0.01 b/s
MaxCutPool	0.03 b/s	0.10 b/s	0.01 b/s	0.09 b/s	0.13 b/s

We note that one-over-K methods such as Graclus, NDP, and k-MIS perform a preprocessing step on the CPU before the training starts. Such operations are not accounted for in the measurements in Tab. 14, but they can take significant time and be a bottleneck in those cases that require operations such as eigenvalues decomposition.

F.3 Memory usage

~~In Figure~~

Table 15: Average and maximum GPU memory usage (in MB) by the architecture for node classification when configured with different pooling methods.

	Roman-e.		Amazon-r.		Minesw.		Tolokers		Questions	
Pooler	Avg.	Max	Avg.	Max	Avg.	Max	Avg.	Max	Avg.	Max
Diffpool	7167.3	11277.2	8367.8	13165.6	1397.4	2199.4	1931.	3039.7	OOM	OOM
DMoN	5301.9	7359.5	6189.5	8591.2	1035.1	1438.2	1429.	1984.7	OOM	OOM
MinCutPool	7167.8	11277.6	8367.9	13165.8	1398.0	2200.3	1932.	3040.0	OOM	OOM
~~Top-k~~	~~2.8~~	~~3.9~~	~~3.4~~	~~4.9~~	~~1.4~~	~~1.8~~	~~3.4~~	~~6.0~~	~~5.1~~	~~8.9~~
Graclus	2.5	2.6	4.0	4.1	1.5	1.5	14.6	15.1	10.4	10.6
k-MIS	1.3	1.3	0.7	0.8	0.3	0.3	2.4	2.5	5.2	5.3
NDP	1.8	2.5	1.8	9.7	0.6	2.5	2.4	70.8	2.4	26.1
MaxCutPool	13.7	25.7	16.8	31.2	6.9	12.7	27.9	52.2	32.6	61.6

In Tab. 15 we report the average and maximum GPU VRAM used by the architecture for node classification on the different datasets. As for the time, the values reported for Graclus, NDP, and k-MIS do not include the `SEL` and `CON` operations performed in preprocessing.

To give a more interpretable demonstration of how the space complexity scales for the different pooling methods, in Fig. 11 we report the GPU VRAM usage of the different poolers ~~. This has been evaluated on~~ when processing a randomly generated Erdős-Renyi ~~graphs with a~~ graph of increasing size. All the graphs are generated keeping at 0.01 ~~probability of connection. The GPU VRAM usage of the different poolers.~~ the probability of having an edge between any pair of nodes.

The plot shows that in soft-clustering methods the GPU VRAM usage grows exponentially with the graph size. On the other hand, for scoring-based methods, including the proposed MaxCutPool, the growth is sublinear, making these approaches extremely suitable for working with large graphs.

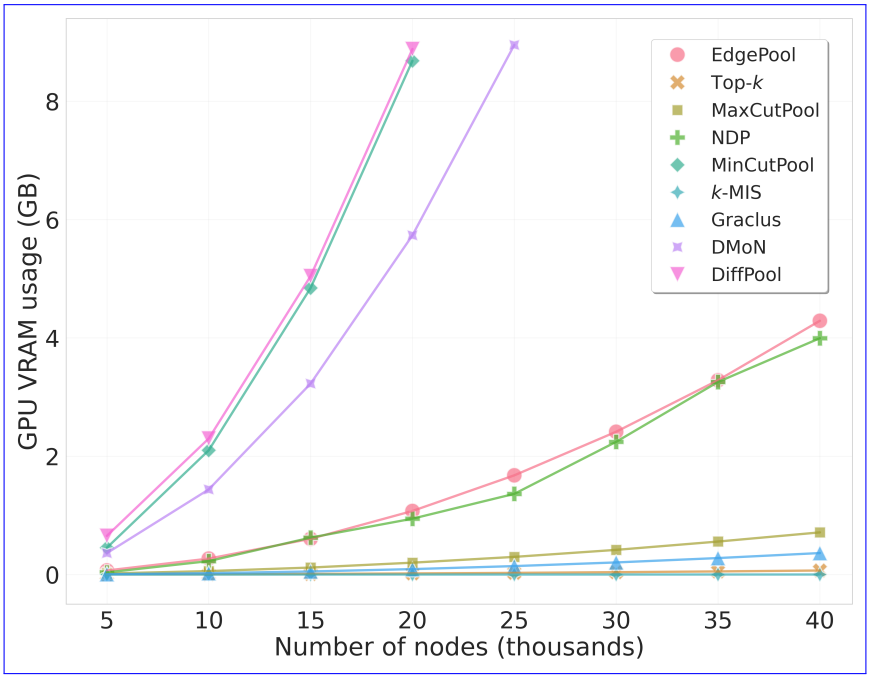

Figure 11: The GPU VRAM usage of the different poolers.